Acta Biomaterialia 10 (2014) 1771–1792

Contents lists available at ScienceDirect

Acta Biomaterialia

journal homepage: www.elsevier.com/locate/actabiomat

Review

The use of physiological solutions or media in calcium phosphate synthesis and processing

A. Cuneyt Tas *

Department of Materials Science and Engineering, University of Illinois, Urbana, IL 61801, USA

ARTICLE INFO

Article history:
Received 12 August 2013
Received in revised form 2 December 2013
Accepted 17 December 2013
Available online 31 December 2013

Keywords:
Physiological media
Calcium phosphate
Synthesis
Biomimetic

ABSTRACT

This review examined the literature to spot uses, if any, of physiological solutions/media for the in situ synthesis of calcium phosphates (CaP) under processing conditions (i.e. temperature, pH, concentration of inorganic ions present in media) mimicking those prevalent in the human hard tissue environments. There happens to be a variety of aqueous solutions or media developed for different purposes; sometimes they have been named as physiological saline, isotonic solution, cell culture solution, metastable CaP solution, supersaturated calcification solution, simulated body fluid or even dialysate solution (for dialysis patients). Most of the time such solutions were not used as the aqueous medium to perform the biomimetic synthesis of calcium phosphates, and their use was usually limited to the in vitro testing of synthetic biomaterials. This review illustrates that only a limited number of research studies used physiological solutions or media such as Earle's balanced salt solution, Bachra et al. solutions or Tris-buffered simulated body fluid solution containing 27 mM HCO_3^- for synthesizing CaP, and these studies have consistently reported the formation of X-ray-amorphous CaP nanopowders instead of Ap-CaP or stoichiometric hydroxyapatite (HA, $Ca_{10}(PO_4)_6(OH)_2$) at 37 °C and pH 7.4. By relying on the published articles, this review highlights the significance of the use of aqueous solutions containing 0.8–1.5 mM Mg^{2+}, 22–27 mM HCO_3^-, 142–145 mM Na^+, 5–5.8 mM K^+, 103–133 mM Cl^-, 1.8–3.75 mM Ca^{2+}, and 0.8–1.67 mM HPO_4^{2-}, which essentially mimic the composition and the overall ionic strength of the human extracellular fluid (ECF), in forming the nanospheres of X-ray-amorphous CaP.

1. Extracellular fluid (ECF) of the human body

Water, being vital for all forms of life, covers approximately 70% of the earth's surface, but only 2.5% of this vast amount of water is fresh water. 98.8% of the global fresh water reservoir is contained in ice and groundwater [1]. Water is the main component of biomineralization media in which almost all biological reactions leading to hard tissue formation or ossification takes place [2–4]. Although fresh water is essential to animals and plants, the physiological fluids of animals, which take part in biomineralization events, are not high-purity water. Water in its purest form is an abstraction and is hard to find in earth's aquifers. In laboratory experiments and in most industrial-scale applications, researchers and technicians use distilled, deionized or critical laboratory reagent grade (CLRW) water. According to the definition of Barskov [5], biological mineralization is the coevolution of the biological and mineral worlds. Biological molecules resulting from the normal or pathological metabolism of organisms and the inorganic ions present in their operational environment forming the mineral world interact to create the mineralized tissues of humans, animals and plants [5]. The inorganic ions, such as Ca^{2+}, Mg^{2+}, Na^+, K^+, HPO_4^{2-} (monohydrogen phosphate), HCO_3^- (bicarbonate), Cl^- and SO_4^{2-}, present in biological fluids and cells play a crucial role in the formation of ion-substituted calcium phosphates of hard tissues at the nanoscale. As such, nanotechnology has been with us in its most sophisticated forms (e.g. in the tissues of living creatures) for billions of years much before the invention of this word in 1974 [6].

Physiological fluids of humans can be viewed in two major compartments: intracellular fluid (ICF, with a volume of 27 l for a 70 kg person) and extracellular fluid (ECF, 13 l). Extracellular fluid is then divided into two sub-compartments, interstitial fluid (ISF, 9.5 l) and the liquid component of blood (plasma, 3.5 l for a 70 kg person). ECF represents the fluid outside cells whereas ICF is the fluid within cells. ISF is the tissue fluid found between cells. Plasma contains significantly more protein than does ISF, and the plasma proteins are the only constituents of plasma that do not cross into ISF [7]. There is a striking difference between the compositions of intracellular and extracellular fluids, as shown in Table 1 [8]. The composition of blood plasma is similar to that of ECF [9]. In brief, the plasma membrane of cells is freely permeable to water and

* Tel.: +1 979 633 8064.
E-mail address: c_tas@hotmail.com

1742-7061/$ - see front matter © 2013 Acta Materialia Inc. Published by Elsevier Ltd. All rights reserved.
http://dx.doi.org/10.1016/j.actbio.2013.12.047

Table 1
Electrolyte composition of ICF and ECF compartments (in mM).

	Na^+	K^+	Mg^{2+}	Ca^{2+}	HPO_4^{2-}	HCO_3^-	Cl^-	SO_4^{2-}
ICF	10	140	29	0.01	37	10	4	1
ECF	142	5	1.5	2.5	1	27	103	0.5

impermeant to ions other than through ion channels. For instance, NaK-ATPase (the enzyme that splits adenosine triphosphate) is an ion channel, which actively moves K^+ into the cell and removes Na^+ out to maintain the ionic concentrations shown in Table 1 within narrow limits [8].

There is a significant difference between the Ca^{2+} concentrations of intracellular (0.01 mM) and extracellular fluids (2.5 mM). The calcium ion is, pharmacologically, one of the most disruptive substances for normal cell function, with the intracellular concentration of calcium ions carefully regulated [10] and the bones serving as the major storage sites for excess calcium. Based on the accurate elemental analysis of bone and tooth specimens recently given by Castro [11], human bones contain 24.5 wt.% Ca, 11.5% P, 5.8% CO_3, 0.7% Na, 0.55% Mg and 0.03% K, besides a number of trace elements at the ppm level, including Zn, Fe, Sr, Pb, Ba and Cu. Carbonate, sodium, magnesium and potassium ions are the major dopants of apatitic calcium phosphate (Ap-CaP) bone mineral, and the same ions are also present in ECF. The carbonated, ion-substituted, non-stoichiometric and cryptocrystalline Ap-CaP inorganic phase (i.e. biological apatite) of bones in fact stores 99 wt.% of the body's calcium, 80 wt.% of its phosphorus and 50 wt.% of its magnesium [12–14]. In other words, as a toxic ion that needs to be removed from most cells, calcium accumulates extracellularly and the occurrence of calcium deposits may therefore represent a form of detoxification [10,15]. Simkiss [15] briefly described biomineralization as a cellular detoxification mechanism. This review searches the previous literature for solutions mimicking extracellular fluid and their use in synthesizing calcium phosphates.

2. Biomimetic synthesis

The phrase "biomimetic synthesis", according to the Web of Knowledge[SM] database, was first used in 1972 to describe specific synthesis protocols for nicotine [16], macralstonine [17] and villalstonine [18]. Biomimetic synthesis was, therefore, not historically coined for the production of synthetic biomaterials of tissue engineering. Tabushi and Imuta [19] mentioned the biomimetic synthesis of nucleotide phosphates in 1982. Nucleotides are biological molecules that form the building blocks of the nucleic acids DNA and RNA. Abe et al. [20] developed a biomimetic process to deposit a layer of cryptocrystalline apatitic calcium phosphate on ceramics, metals and polymers immersed, at 36.5–37 °C, in what they called the simulated body fluid (SBF). Mann [21] summarized the biomimetic approaches in inorganic materials chemistry until 1993. However, the examples provided in Mann's article [21] did not show any material synthesis procedures pursued in aqueous media with compositions similar to that of the ECF given in Table 1.

Extracellular fluid is supersaturated with respect to the formation of carbonated (6 wt.% of bones), ion-substituted, non-stoichiometric biological apatite, and the presence and action of biochemical inhibitors of nucleation/crystallization prevents our bodies from being mineralized all over [22]. Blood is circulated in the entire human body, by flowing through the total length of approximately 100,000 km (one hundred thousand kilometers) of veins and capillaries, just to make its inorganic and organic constituents instantly available to the hard and soft tissues, which need to undergo continuous renovation and renewal. This is an outstanding example, given by the human metabolism, to explain the meaning of bioavailability. Calcium phosphate syntheses performed in non-replenished and constant volume batches of distilled/deionized water, which are prone to suffer from the depletion of the initial ions upon the start of precipitation, obviously contradict the scale of bioavailability (of ECF) exemplified by the human metabolism.

Sarikaya and Aksay [23,24] divided biomimetic technology into two categories, i.e. biomimicking (imitating the unique physicochemical and structural design of biomaterials by using the currently available techniques) and bioduplication (mastering the molecular synthesis and processing mechanisms of biological materials to produce new and superior biomaterials), and thus helped to set the roadmap for future research initiatives at the junction of materials science and biology, albeit without mentioning the role of Na^+, Mg^{2+}, Sr^{2+}, SO_4^{2-} and Cl^- present in sea water on mineralization when citing examples on biomineralization of sea urchins and seashells.

Going through the abundant literature related to the synthesis of calcium phosphates in distilled or deionized water has been kept outside the scope of the current review. However, readers may consult the review articles, just to name a few, of Dorozhkin [25,26], Boanini et al. [27], Bleek and Taubert [28], Omelon and Grynpas [29], Wang and Nancollas [30], Coelfen [31], Alves et al. [32], Boskey [33], Addadi and Weiner [34], Habibovic and Barralet [35], Bose and Tarafder [36], Sadat-Shojai et al. [37], and Gomez-Morales et al. [38] for that purpose.

The early, yet quite influential, work of the pioneering calcium phosphate (CaP) researchers, such as Hayek et al. [39,40], Posner et al. [41,42] and Jarcho et al. [43], used distilled water as the synthesis medium and added to it one of the soluble salts of calcium (such as anhydrous $CaCl_2$ (extremely hygroscopic), $CaCl_2{\cdot}2H_2O$, $CaCl_2{\cdot}6H_2O$, $Ca(NO_3)_2{\cdot}4H_2O$ or $Ca(CH_3COO)_2{\cdot}H_2O$) and a water-soluble salt of phosphate (selected from one or more of $(NH_4)_2HPO_4$, $NH_4H_2PO_4$, Na_2HPO_4, $NaH_2PO_4{\cdot}H_2O$, K_2HPO_4 or KH_2PO_4) to induce the precipitation of apatitic CaPs. Such early work, with the notable exception of that of LeGeros et al. [44], did not introduce HCO_3^- ions into the synthesis solutions despite the well-known carbonated nature of bone apatite (5.8 wt.% carbonate). Bone marrow and bones (and most human tissues except hairs and nails) are soaked in blood, not water. Similarly, the external surfaces (whether they are enamel or dentine) of teeth are continuously soaked in saliva but not water.

Early works [39–43] did not mention the possibility of contaminating the Ap-CaP precipitate surfaces with ammonium ions during syntheses, especially when using ammonium phosphate salts, which was shown to be possible much later by the work of Ivanova et al. [45]. Habelitz et al. [46] showed that it would be possible to incorporate nitrogen (even at the wt.% levels) into the lattice of calcium-deficient Ap-CaP at a temperature as low as 800 °C when the heat treatment is performed in an ammonia atmosphere. The earlier articles of the present author on the biomimetic synthesis of Ap-CaP in solutions similar to the ECF also falls in this category since the solutions contained ammonium and nitrate ions which are not present in the ECF [47–50]. The lattice of Ap-CaP is quite accommodating for a significant number of diverse ions (including heavy metals such as lead) present in aqueous solutions in which it was synthesized, as shown in the work of Bigi et al. [27,51,52] and Verbeeck et al. [53].

The majority of published articles related to the synthesis of Ap-CaP [25–38] did not use the main component of blood plasma, i.e. NaCl, in the synthesis solutions, despite Ringer's previous work to that effect [54–56]. On the other hand, when geologists, geochemists and micro- or marine biologists studied the in vitro biomineralization of $CaCO_3$ (calcite, aragonite or vaterite) or apatite, they usually took note of the "salinity" of their mineralization media

[57–62]. The introduction of biologically relevant ions, e.g. Na^+, K^+, Cl^-, SO_4^{2-}, HCO_3^- and Mg^{2+}, at levels close to those present in ECF for CaP synthesis alters the ionic strength of the synthesis solutions, which is explained below.

Biomimetic or biomimicking CaP synthesis processes require solutions similar to ECF. Such synthetic solutions similar in composition to ECF (as listed in Table 1) may also contain biomolecules present in ECF. Biomimetic CaP synthesis is performed at physiological temperature (37 °C) and pH (7.4). As such, the term biomimetic refers to the chemical similarity of the synthesized CaP to the biological CaP of the bone mineral.

In preparing a synthetic aqueous solution mimicking the ECF composition shown in Table 1, one uses the following inorganic chemicals of the highest possible purity: NaCl, KCl, $MgCl_2{\cdot}6H_2O$, $CaCl_2{\cdot}2H_2O$ or $CaCl_2{\cdot}6H_2O$, Na_2HPO_4 or $Na_2HPO_4{\cdot}2H_2O$, $NaHCO_3$ and Na_2SO_4. The pH of such a precipitate-free solution can be adjusted to physiological pH at physiological temperature by using small amounts of, for instance, the pair of Na-L-lactate powder and 1 M lactic acid solution [63,64]. Lactated Ringer's solution (RLS), which is used today in hospitals for intravenous or subcutaneous administration, will be briefly mentioned later in this review.

The ionic strength (I) of an ECF-mimicking solution is calculated as shown in Eq. (1), using the formula of Debye and Hückel [65]. One simply enters into this formula the concentrations of ions (in M, moles/L) and the valency of ions. The value of the ionic strength (expressed in molarity, M or mM) then serves as a reliable numerical index for exchange between researchers using and/or developing different biomineralization media based on their specific research needs.

$$\begin{aligned} I = 1/2[&(2.50\times10^{-3})^{Ca^{2+}}(2)^2 + (1.42\times10^{-1})^{Na^{+}}(1)^2 + (1.0\times10^{-3})^{HPO_4^{2-}}(2)^2 \\ &+ (1.03\times10^{-1})^{Cl-}(1)^2 + (2.7\times10^{-2})^{HCO_3^-}(1)^2 + (5\times10^{-3})^{K+}(1)^2 \\ &+ (1.5\times10^{-3})^{Mg^{2+}}(2)^2 + (5\times10^{-4})^{SO_4^{2-}}(2)^2] = 0.1495\ \text{M} \end{aligned} \quad (1)$$

Marques et al. [66] showed the release of CO_2 (g) from an aqueous solution containing bicarbonate ions (HCO_3^-) would occur at a faster rate if the solution has a low ionic strength. If one increases the ionic strength of a metastable, supersaturated calcium phosphate solution to much higher values, such as 0.6 M [67] or 1.1 M [68], its rate of CO_2 release decreases further. The ionic strength of an ECF-like bicarbonate ion-containing solution (at 27 mM; see Table 1) is thus quite important for the biomimetic synthesis of carbonated Ap-CaP.

Habibovic et al. [69] noted that the presence of 1.5 mM Mg^{2+} in biomineralization media could be effective in suppressing the growth of well crystallized Ap-CaP, favoring instead the formation of nanocrystalline, carbonated, hydroxyl-deficient and large surface area Ap-CaP similar to the mineral phase of younger bones [14,70–76]. Alfrey et al. [77] have found that bone magnesium was falling with age, in a study performed with rats, and concluded that, since the plasma magnesium content was not different in the various age groups examined, the most likely reason for that fall was the growth of bone crystal size with age associated with a decrease in the surface area of crystals. Robinson and Watson [70] reported that the newly formed bone has a smaller crystal size and a larger surface area. Not only does the presence of Mg^{2+} have an inhibitory effect on the crystallization of apatite; the presence of 0.15 M NaCl (ECF contains an amount of NaCl roughly similar to this value) in an aqueous synthesis solution, such as the one used by Nancollas and Tomazic [78] in 1974, was also found to noticeably decrease the crystallization rate of Ap-CaP.

Bell et al. [79], in 1973, experimentally confirmed that when NaCl was used as a supporting electrolyte, some of the Ca^{2+} ions on the surfaces of Ap-CaP were exchanged by Na^+ ions. The similarity of the ionic radii of Ca^{2+} (114 pm) and Na^+ (116 pm) makes this exchange feasible. The Bell et al. [79] study underlined the influence of the salinity of the medium on biomimetic CaP synthesis. Drouet et al. [80] have shown that a similar exchange can take place between the surface Ca^{2+} ions of nanocrystalline apatite and Mg^{2+} (ionic radius of 86 pm) present in maturation solutions into which the apatite powders were immersed.

The separate work of LeGeros [44] on the influence of carbonate ions, those of Bell et al. [79] and Nancollas and Tomazic [78] on the influence of NaCl, and those of Habibovic et al. [69] and Drouet et al. [80] on the influence of magnesium ions in the synthesis media independently defined the outline of synthesizing carbonated, ion-substituted and biomimetic Ap-CaP. Therefore, CaP synthesis, for instance, by the routes of $Ca(OH)_2$–H_3PO_4 or $Ca(NO_3)_2{\cdot}4H_2O$ (or $CaCl_2{\cdot}2H_2O$)–$(NH_4)_2HPO_4$ in deionized water, devoid of Na^+, Mg^{2+} and HCO_3^- ions, represent deviations from the biomimetic approach, but these routes are able to produce apatite of relatively high purity [81]. On the other hand, biological bone apatite is not stoichiometric calcium hydroxyapatite (HA, $Ca_{10}(PO_4)_6(OH)_2$) [14].

CaO–P_2O_5–CO_2–H_2O system is one of the richest of all the inorganic material systems, and allows the synthesis of amorphous calcium phosphate (ACP), cryptocrystalline calcium phosphate (apatitic CaP of poor crystallinity) or well-crystallized calcium phosphate (e.g. brushite, $CaHPO_4{\cdot}2H_2O$, dicalcium phosphate dihydrate) phases at temperatures well below 90 °C. ACP is denoted by the formula $Ca_x(PO_4)_y{\cdot}nH_2O$, which indicates a phase of uncertain composition and non-crystalline structure [27], and its formation was correlated to the Posner's clusters of 0.85–0.95 nm diameter present in supersaturated and metastable calcium phosphate solutions [82–85]. The role played by Mg in stabilizing X-ray-amorphous calcium phosphate was previously explained by Posner et al. [86,87]. It is clear that studies focusing solely on stoichiometric HA will not be sufficient to understand the full complexity of biological calcium phosphates of bones, teeth, kidney stones, articular cartilage, mitral valves or dental calculi.

The synthesis of fully stoichiometric hydroxyapatite samples with no deficiency in the Ca^{2+} and OH^- sites, with a Ca/P molar ratio of 1.67 and with no HPO_4^{2-} or CO_3^{2-} ions in the lattice) were shown in the authoritative work of Fowler [88–90] to only be possible by heating a gravimetric mixture of $10CaO{\cdot}3P_2O_5$ in steam at 1.5 atm at temperatures from 900 to 1100 °C. Meyer and Fowler [90] were not able to synthesize fully stoichiometric HA even when they tried to produce stoichiometric HA by wet-chemical synthesis at pH 10: their samples were still OH-deficient. The possibility of forming stoichiometric HA in an ECF-like solution (having all ions of ECF at the concentrations stated in Table 1) at 37 °C and pH 7.4 is quite slim, if not impossible. The work of Fowler [88–90] indicates the borderline between the "ceramic synthesis" and "biomimetic synthesis", i.e. if one has a high-temperature furnace and the ability to maintain water vapor in the furnace at above atmospheric pressure while heating the samples, then synthesizing stoichiometric HA is not a difficult task. Therefore, the term "hydroxyapatite" should be used with extreme caution, since bone apatite contains very small amounts of hydroxyl ions [14,22].

3. Collagen fibrils and biomimetic synthesis

The transmission electron microscope (TEM) with a total magnification of about ×17 was first developed in 1932 by Knoll and Ruska [91,92]. Hard tissues (bones and teeth) were among the first materials examined by transmission electron microscopy (TEM).

Bone and dentin are composite materials composed of water (6 (bone)–10 (dentin) wt.%), collagen fibrils (20 (dentin)–24 (bone)%) and biological nanoapatite (70%) [22]. Biological nanoapatite occupies about 50% of the volumes of bone and dentin [22]. Nanoapatitic crystals of bones were imaged in the 1950s by using TEM. Collagen fibrils were observed to have a width of approximately 80 nm [93,94]. Collagen fibrils displayed unusual bands with an almost constantly repeating period spacing of 67 nm, which was called a collagen banding (or cross-striated) pattern [93,94]. Rouiller et al. [95] studied the structure of dentin using an electron microscope in 1952. These quite exciting early discoveries revealed that bone, which is mechanically strong yet resilient, consists of delicately intervowen collagen fibrils embedded with biological nanoapatites. This brief section of this review will try to answer the following question: where does one stand now in terms of the biomimetic synthesis of collagen–calcium phosphate hybrids by using biomineralization solutions or media similar in composition to the extracellular fluids?

It seems like most research adopted rapid approaches to produce collagen-calcium phosphate hybrids within short hours, rather than trying to:

(i) understand how a 50 nm-large biological, significantly (5.8 wt.%) carbonated, ion-substituted (Na^+, Mg^{2+} and K^+ summing up to 1.28 wt.%), hydrous, and hydroxyl-deficient apatitic particle (formed out of ECF) aligns itself along the inherent and constant period-spacing bands of collagen fibrils or
(ii) explain how a collagen fibril accommodates and orients biological nanoapatite particles onto itself in ECF.

Modern research, with its easy access to powerful electron and atomic force microscopes, seems to have focused on rapid techniques, which precipitated significant quantities of aggregated apatitic calcium phosphate nano- or microparticles onto the collagen fibrils in a short period of time (produced in Mg^{2+}-, SO_4^{2-}-, and HCO_3^--free water solutions). Martin and Brown [96] specifically studied the effect of Mg^{2+} on Ap-CaP formation in water at 37.4 °C. Eanes and Hailer [97] provided comprehensive evidence on how these ions affected the crystal size and shape of apatites. Most of the current collagen–apatite hybrid research, which is reviewed below, treated collagen fibrils only as mock templates (or as secondary heterogeneities that happen to be present in the solution) onto which the solid precipitates separating from the solution settled down.

The H_3PO_4–$Ca(OH)_2$ acid–base neutralization reaction, being a well-established technique to synthesize pure CaPs, is used in most research to produce collagen–CaP composites [98–106]. Another preferred approach to produce such composites was the addition of externally synthesized apatite powders to an aqueous suspension having solubilized collagen in it. This technique was adopted from the conventional ceramic processing method that has been used for producing ceramicware for over millennia [107–122]. A significant number of studies have employed precipitation techniques based on picking one of the high-solubility salts of calcium, such as Ca-chloride, Ca-nitrate, Ca-acetate or Ca-hydroxide, and reacting it with a Na-phosphate, K-phosphate or ammonium phosphate salt in a collagen-containing water solution, again free of Mg^{2+}, HCO_3^- and SO_4^{2-} ions [13,96,97]. In these approaches the pH of the solution is adjusted, when required, by adding aliquots of NaOH or NH_4OH in order to prevent the precipitation of brushite or octacalcium phosphate ($Ca_8(HPO_4)_2(PO_4)_4{\cdot}5H_2O$) [123–133]. Some molecular simulation attempts have tried to visualize collagen–HA hybrid in pure water by using only Ca^{2+}, PO_4^{3-} and OH^- ions, without taking into account the roles of other biologically relevant ions present in the ECF in forming biological apatites [134,135]. A small number of studies experimented with the presence of, for example, poly L-aspartic acid (which was used as an oversimplified model of acidic noncollagenous proteins) in processes to precipitate CaP onto collagen fibrils, although the influence of Mg^{2+} and HCO_3^- ions on the mineralization of biological apatites [136–140] was not given due consideration.

The technique of immersing collagen matrices into an SBF [20] solution at physiological temperature set itself apart from the above bulk precipitation techniques as the acellular SBF solutions try to imitate the inorganic ion concentrations of the ECF. SBF-based collagen-coating studies were able to generate CaP layers with physical chemical properties (i.e. carbonated, ion-substituted, non-stoichiometric and hydrous) more similar to those of biological apatites on the collagen fibrils [141–145]. One should note here that, while SBF solutions that are HCO_3^--deficient (i.e. 4.2 mM [20]) deposited apatitic CaP globules >1 μm in diameter and were not able to cover the entire surfaces of the collagen fibrils [141,143], an SBF solution achieving the physiological HCO_3^- concentration (i.e. 27 mM [47,48]) coated the collagen matrix surface entirely and the diameters of the apatitic CaP globules were smaller than 1 μm [142]. The role of HCO_3^- and Mg^{2+} concentrations in a biomimetic solution, such as SBF, in affecting the nature of CaP precipitation has been described by Barrere et al. [146] and confirms the above difference observed in collagen matrix/sponge immersion experiments performed by SBFs differing in their bicarbonate contents.

The technique of mineralization reported by Nudelman et al. [140] differs from the techniques of the majority of other studies cited in this section [98–145], particularly in its way of execution (perhaps due to the advantageous use of cryoTEM), in that amorphous calcium phosphate (ACP, $Ca_x(PO_4)_y{\cdot}nH_2O$) was observed to form and enter into the collagen fibrils. Nudelman et al. [140] also claimed, with convincing experimental support coming from their high-resolution cryoTEM images, that mineralization occurred exclusively inside the fibrils, with Ap-CaP crystals then forming from that ACP precursor. Furthermore, the much earlier work of Hohling et al. [147,148] had already reported dot-like, amorphous-looking CaP nuclei with diameters in the vicinity of 3 nm (similar to those synthesized by Nudelman et al. [140]), mineralizing within human collagen fibrils.

The rest of the studies cited in this section were not able to detect and report the initial stage(s) of mineralization since they were mostly aimed at blending HA nanocrystals with collagen fibrils. The nucleation of crystalline Ap-CaP in aqueous solutions is preceded by the formation of ACP. Abbona and Baronnet [149], Brecevic et al. [150] and Christoffersen et al. [151] reported such early forming (i.e. within the first few minutes of synthesis) ACP nanoparticles by using TEM. If such early forming ACP nanoparticles were not intentionally stabilized by adding Mg^{2+}, pyrophosphate ($P_2O_7^{4-}$) [84,152] or carbonate (HCO_3^-) ions to the synthesis media, then they transformed into crystalline octacalcium phosphate and/or non-stoichiometric Ap-CaP with an increase in aging time, even in their native precipitation solutions [153–161]. Hohling et al.'s [147,148] studies from the 1970s, which detected very small ACP nuclei forming on collagen fibrils, are again of significant importance today thanks to the recent reminder given by Nudelman et al. [140].

A few procedures for the preparation of biomimicking solutions are provided in Table 2. These solutions [162] were named saline ionic essentials medium (SIEM), and can be prepared in two different versions: as SIEM-*n*, which is a solution of neutral pH (7–7.5), and as SIEM-*b*, which is a basic solution of pH 12. Both solutions, which are calcium- and phosphorus-free, are quite simple to prepare. If the strict prevention of bacterial growth (due to contamination from the ordinary laboratory environment) in the SIEM-*n* solution becomes an issue, then one may easily dissolve 100 mg l^{-1} NaN_3 (sodium azide) in the solution during its preparation. SIEM-*n*

Table 2
Examples of simple solutions partially mimicking the inorganic ion composition of ECF (ion concentrations are in mM) [162].

Solution	Na^+	K^+	Mg^{2+}	Ca^{2+}	HPO_4^{2-}	HCO_3^-	Cl^-	SO_4^{2-}	Chemical (g l^{-1})	SIEM-*n*	SIEM-*b*	Amor-CaP	Crypt-CaP
SIEM-*n*	123	5	1.5	–	–	27	103	0.5	NaCl	5.552	5.552	5.552	5.552
SIEM-*b*	142	5	1.5	–	–	–	103	0.5	KCl	0.373	0.373	0.373	0.373
Amor-CaP	133	5	1.5	12.5	5	27	103	0.5	$MgCl_2{\cdot}6H_2O$	0.305	0.305	0.305	0.305
Crypt-CaP	133	5	1.5	12.5	5	27	128	0.5	$NaHCO_3$	2.268	–	2.268	2.268
									Na_2SO_4	0.071	0.071	0.071	0.071
									Na_2HPO_4	–	–	0.710	0.710
									NaOH	–	1.840	–	–
									Ca metal	–	–	0.501	–
									$CaCl_2{\cdot}2H_2O$	–	–	–	1.838

contains HCO_3^- at the concentration identical to that of ECF, whereas the SIEM-*b* solution is carbonate-free but matches the ion concentrations of ECF perfectly.

SIEM-*n* and SIEM-*b* solutions (or volumetric mixtures thereof to further adjust their Na^+ (i.e. $123 < Na^+ < 142$) and HCO_3^- ($0 < HCO_3^- < 27$) concentrations) can, for instance, be used for soaking (at 37 °C) the collagen matrices or fibrils prior to calcification/mineralization with the purpose of impregnating their surfaces with the biologically relevant ions the solutions contain. Such studies are absent in the relevant literature. Pre-boiled, 18.2 MΩ deionized water and chemicals of the highest possible purity should be used in preparing the SIEM-*n* and SIEM-*b* solutions. These solutions may help to inspire research using simple-to-prepare physiological media. SIEM-*n* and SIEM-*b* solutions can also be used, for instance, for the quantitative determination of the amounts of Ca^{2+} and/or HPO_4^{2-} ions leached out from soluble CaPs or bioglasses under biomimicking conditions.

SIEM-*n* and SIEM-*b* are not calcification solutions, though the solutions named as Amor-CaP and Crypt-CaP in Table 2 [162] are modified SIEM solutions with the power of calcification/mineralization of either amorphous CaP or cryptocrystalline CaP. In the case of 1 l of Amor-CaP solution (which contains 5 mM HPO_4^{2-}), if one adds 0.501 g of Ca metal (12.5 mM) into the solution at the last step [162], followed by 30 min of mild stirring at 37 °C and pH 10, amorphous CaP nanoparticles form, as shown in the scanning electron microscopy (SEM) photomicrograph of Fig. 1a. On the other hand, if one adds 1.838 g (12.5 mM) of $CaCl_2{\cdot}2H_2O$ to 1 l of Crypt-CaP solution (which also contains 5 mM HPO_4^{2-}) at the last step, followed by 30 min of mild stirring at 37 °C and pH 7 [162], nanoparticles of cryptocrystalline CaP form, as shown in Fig. 1b. Figs. 1a and 1b were recorded at the same magnification [162]. The pH values mentioned above were autogenous and did not involve any base/acid additions to the solutions during mineralization. These procedures can serve as simple examples for converting the SIEM-*n* solution into a mineralization/calcification solution(s).

In summary, the success of the biomimetic synthesis of load-bearing calcium phosphate–collagen hybrids presently seems to depend on (i) the hierarchical formation of ACP nanoparticles on or along the collagen fibrils (the work of Hohling et al. [147,148]) and (ii) the proper inhibition of the growth of nanoparticles and the minimization of nanoparticle aggregation (the work of Fleisch [152]). More studies like that of Reid et al. [163] will surely be needed to determine (and learn from) the role played, for instance, by sugars such as glycosaminoglycans in limiting the calcium phosphate biomineralization at the organic fibril–calcium phosphate interface on the nanoscale architecture of biological collagen fibrils, as originally observed in the 1950s.

4. Ringer's physiological saline and lactated Ringer's solution

The classical literature (from the 1880s to the 1960s) is rich in significant publications on the formulation or development of precipitate-free calcification or biomineralization solutions mimicking the compositions of physiological fluids, concurrent with advances in cell biology within the same timeframe. These solutions are reviewed in this and the following sections.

Most contemporary bioceramic research (from the 1960s to date) did not initially set its purpose to devise a bioceramic synthesis process that starts with a precipitate-free (to the naked eye) aqueous mother liquor which is supersaturated with respect to the precipitation of Na^+-, K^+-, Mg^{2+}-, Zn^{2+}-doped, carbonated and, as a consequence, calcium- and OH^--deficient para- or cryptocrystalline Ap-CaP. Most contemporary research has refrained from using a simple saline, such as the Ringer's physiological saline [54–56], as its main synthesis medium. This review will, therefore, look at the gap between today's CaP research, which employs high-purity water in syntheses rather than biomineralization or physiological salines, developed almost 60 to 130 years ago.

Ringer experimented with the effects of various constituents of blood on the contractions of the frog's excised heart and conducted

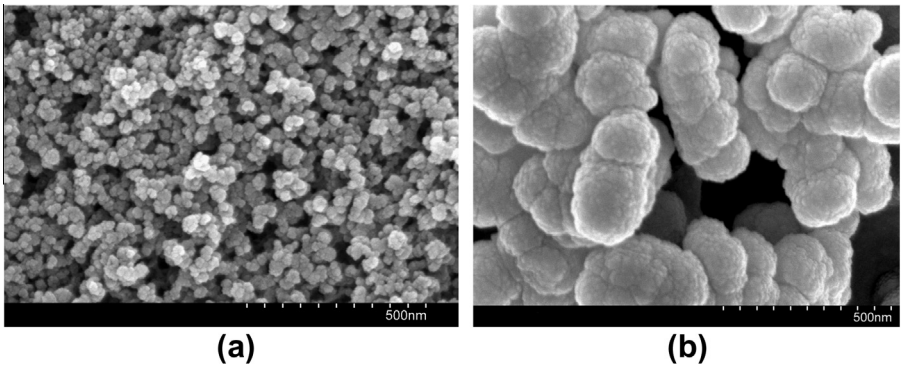

Fig. 1. SEM photomicrographs of samples synthesized in the (a) Amor-CaP and (b) Crypt-CaP solutions of Table 2.

Table 3a
Compositions of ECF vs. inorganic physiological/biomineralization media (ions in mM).

	Na^+	K^+	Mg^{2+}	Ca^{2+}	HPO_4^{2-}	HCO_3^-	Cl^-	SO_4^{2-}
ECF [9]	142	5	1.5	2.5	1	27	103	0.5
Ringer [54–56]	113.6	1.88	–	1.08	–	2.38	115.3	–
Locke [168]	156.38	5.63	–	2.16	–	2.38	163.95	–
Ringer lactate [164]	130.66	4.02	–	1.4	–	–	109.48	–
Tyrode [198]	149.12	2.68	0.53	1.8	0.33	11.9	144.23	–
KHB [199]	143.4	5.88	1.25	2.52	1.18	25	128.2	1.25
EBSS [200]	143.6	5.37	0.83	1.8	1.04	26.2	125.3	0.83
HBSS [208]	141.6	5.81	0.81	1.26	0.78	4.065	144.8	0.81
Eagle's MEM [264]	140.9	5.4	1	1.8	1.1	23.8	126	–
DMEM [268]	127	5.33	0.81	1.8	0.906	44.05	90.8	–
ACP [270]	127	5.33	0.81	2.262	0.906	44.05	93.4	–
Bachra [292,294]	145	5	0–10	3.75	1.67	22–110	133	–
SBF [20]	142	5	1.5	2.5	1	4.2	147.8	0.5
SBF-T [47,48]	142	5	1.5	2.5	1	27	125	0.5
SBF-H [325]	142	5	1.5	2.5	1	27	103	0.5
SBF-L [64]	142	5	1.5	2.5	1	27	103	0.5
Synthetic urine [395]	111.09	42.04	3.2	4.43	20.58	–	134.12	16.19
Artificial saliva [400]	11.88	5.36	–	5.41	5	–	23.02	0.02

(1) RLS also contains 28 mM Na-L-lactate ($NaCH_3CH(OH)COO$); HBSS contains 0.42 mM Na_2HPO_4 and 0.44 mM KH_2PO_4; DMEM and Eagle's MEM solutions also contain amino acids, vitamins and glucose (not shown here); the synthetic urine recipe also contains 18.69 mM NH_4Cl, 416.3 mM urea, 1 g l^{-1} creatinine and 10 g l^{-1} tryptic soy broth; the artificial saliva formulation contains 0.02 mM $Na_2S{\cdot}9H_2O$ and 1 g l^{-1} urea.
(2) KHB: Krebs–Henseleit buffer; EBSS: Earle's balanced salt solution; HBSS: Hanks' balanced salt solution; ACP: amorphous calcium phosphate solution; SBF: simulated/synthetic body fluid; SBF-T: SBF–50 mM Tris–27 mM HCO_3; SBF-H: SBF–50 mM HEPES–27 mM HCO_3; SBF-L: SBF–22 mM Na-L-lactate–27 mM HCO_3.

Table 3b
Preparation details of select inorganic physiological/biomineralization media (amounts in g l^{-1}).

	Ringer	Locke	RLS	Tyrode	KHB	EBSS	HBSS	Eagle	DMEM	ACP	Bachra	SBF	SBF-T	SBF-H	SBF-L
NaCl	6.5	9	6	8	6.92	6.8	8	6.8	4.79	4.79	6.993	8.036	6.546	5.4	5.26
KCl	0.14	0.42	0.3	0.2	0.35	0.4	0.4	0.4	0.397	0.397	0.373	0.225	0.373	0.225	0.373
$CaCl_2$	0.12	0.24	0.155	0.2	0.28	0.2	0.14	0.2	0.2	–	0.416	0.292	–	0.292	–
$CaCl_2{\cdot}2H_2O$	–	–	–	–	–	–	–	–	–	0.332	–	–	0.368	–	0.368
$MgCl_2$	–	–	–	0.05	–	–	–	–	–	–	0.095 to 0.95	–	–	–	–
$MgCl_2{\cdot}6H_2O$	–	–	–	–	–	–	–	0.2	–	0.1655	–	0.311	0.305	0.311	0.305
$MgSO_4$	–	–	–	–	–	0.1	–	–	0.1	–	–	–	–	–	–
$MgSO_4{\cdot}7H_2O$	–	–	–	–	0.15	–	0.2	–	–	–	–	–	–	–	–
Na_2SO_4	–	–	–	–	–	–	–	–	–	–	–	0.072	0.071	0.072	0.071
$NaHCO_3$	0.2	0.2	–	1	2.1	2.2	0.342	2	3.7	3.7	1.85 to 9.24	0.355	2.268	0.74	2.268
Na_2CO_3	–	–	–	–	–	–	–	–	–	–	–	–	–	2.05	–
NaH_2PO_4	–	–	–	0.04	–	0.125	–	–	–	–	–	–	–	–	–
$NaH_2PO_4{\cdot}H_2O$	–	–	–	–	–	–	–	–	0.125	0.125	–	–	–	–	–
$NaH_2PO_4{\cdot}2H_2O$	–	–	–	–	–	–	–	0.15	–	–	–	–	–	–	–
KH_2PO_4	–	–	–	–	0.16	–	0.06	–	–	–	–	–	–	–	–
Na_2HPO_4											0.237				
$Na_2HPO_4{\cdot}2H_2O$	–	–	–	–	–	–	0.06	–	–	–	–	–	0.178	–	0.178
$K_2HPO_4{\cdot}3H_2O$	–	–	–	–	–	–	–	–	–	–	–	0.23	–	0.23	–
Na-L-lactate	–	–	3.138	–	–	–	–	–	–	–	–	–	–	–	2.465
1 M lactic acid	–	–	–	–	–	–	–	–	–	–	–	–	–	–	1.5 ml
Tris	–	–	–	–	–	–	–	–	–	–	–	6.06	6.06	–	–
HEPES	–	–	–	–	–	–	–	5.96	5.96	–	–	–	–	11.93	–
1 M HCl	–	–	–	–	–	–	–	–	–	–	–	40 ml	40 ml	–	–
1 M NaOH	–	–	–	–	–	–	–	–	–	–	–	–	–	0.8 ml	

$CaCl_2{\cdot}2H_2O$, $CaCl_2{\cdot}6H_2O$, $MgCl_2{\cdot}6H_2O$ or $NaH_2PO_4{\cdot}H_2O$ can be used in place of the similar chemicals shown above, upon recalculating the specific amounts.
Lactated Ringer's solution (RLS) contains 28 mM Na-L-lactate (i.e. $NaCH_3CH(OH)COO$).
The inorganic compartment of DMEM solutions contains 1×10^{-4} mM $Fe(NO_3)_3{\cdot}9H_2O$.
Eagle's MEM and DMEM solutions contain amino acids, vitamins and glucose (not shown here); they may or may not be buffered with HEPES.
The numbers in this table are taken from the articles cited in Table 3a for the same solutions shown in the top row.

a number of experiments in an attempt to isolate the individual constituents that were most crucial to sustaining the physiological activity of the heart muscle [56]. Ringer's papers read more like an experimental diary and explanation of experiments performed. His papers should inspire today's graduate students on how to write a laboratory notebook. Throughout his work [54–56], Ringer established the importance of aqueous sodium, potassium, calcium, chlorine and bicarbonate ions in preparing a synthetic saline solution which would eventually be able to maintain the normal heartbeat form [164,165]. A well-written synopsis of Ringer's physiological work is given by Lockwood [166]: "An excised frog's heart ceased to beat and became insensitive to stimulation some 20–30 min after transfer to NaCl isotonic with the blood: but addition of $CaCl_2$ to the solution resulted in the resumption of a spontaneous, though abnormal, beat. The inclusion of KCl neutralized the excessive contracture in the NaCl–$CaCl_2$ mixture and the heartbeat was then normal for some hours. Buffering the medium with $NaHCO_3$ further prolonged the activity of the heart."

Ringer's physiological saline is prepared by dissolving four simple inorganic salts in water: 6.5 g l^{-1} NaCl, 0.14 g l^{-1} KCl, 0.12 g l^{-1}

$CaCl_2$ (can be exchanged with less hygroscopic $CaCl_2{\cdot}2H_2O$) and 0.2 g l^{-1} $NaHCO_3$ [56,166]. Ringer's contemporary, Locke [167], was also developing saline solutions that could keep animal tissues alive. Today, Ringer's physiological saline can also be prepared in deionized water by purchasing ¼–strength tablets carrying his name.[1] In order to prepare full-strength Ringer's saline (with a final pH of 7), one adds eight ¼-strength tablets into 1 l of water. However, upon dissolving eight Ringer tablets in 1 l water, one actually gets the Locke's modification (to the Ringer's saline) [168], with the composition of 9.0 g l^{-1} NaCl, 0.42 g l^{-1} KCl, 0.24 g l^{-1} $CaCl_2$ and 0.2 g l^{-1} $NaHCO_3$, but not the original Ringer's physiological saline. This must be noted as an ambiguity. The compositions of Ringer's and Locke's solutions are given in Table 3.

By the early twentieth century, as knowledge of the fundamentals of diffusion and dissociation of ions developed, the physiological importance of electrolytes to cellular activity was recognized [164,169]. As intravenous crystalloid solutions were developed, Ringer's solution was adapted for this purpose [164]. There have been a number of modifications to the constituents of RLS (also called lactated Ringer's solution), most notably by Hartmann and Senn [170] and Darrow and Yannet [171]. The current composition of "lactated Ringer's injection" is 130 mM Na^+, 4 mM K^+, 1.4 mM Ca^{2+}, 109 mM Cl^- and 28 mM Na-L-lactate, at pH 6.5 [164]. The use of RLS as an adjunct to the use of whole blood for the resuscitation of patients in hemorrhagic shock is well established, in addition to its use in soft tissue injuries, burns and operative trauma [172,173]. On the other hand, Ringer's solution encountered in the CaP-related literature has mostly been limited to its use as a physiological saline for testing the dissolution, stability or degradability (typically at 37 °C) of orthopedic cements [174–180], various CaP bioceramics [181–186] and CaP-coated metals [187–196].

It is not easy to answer the question why research (with the notable exception of MacConaill [197]) does not use Ringer's physiological saline in CaP synthesis as an aqueous synthesis medium in place of distilled or deionized water. There happened to be some confusion regarding the exact compositions of Ringer's saline and lactated Ringer's solution. For example, Jun et al. claimed to use Ringer's solution in both of their studies [182,183], but the solution tabulated did not have the composition of Ringer's solution. Alkhateeb and Virtanen [192], in their study, named a solution containing phosphate and magnesium ions as Ringer's solution, although Ringer's solution does not contain these ions. Rajeswari et al. [187,191] prepared a so-called Ringer's solution which lacked $NaHCO_3$ while having Na^+, K^+ and Ca^{2+} concentrations – rather resembling those of Locke's modification of Ringer's solution. Table 3 is provided to clarify these issues, and the author recommends the comprehensive paper of Lockwood [166] as a reference for the Ringer's physiological saline recipe and its successive derivatives, in case access to original articles of Ringer is a challenge.

5. Metastable calcium phosphate solutions

A summary of the partial history of the development of physiological salines and biomineralization media suitable for the biomimetic synthesis of calcium phosphates and calcium carbonates is given in Tables 3a and 3b.

5.1. Tyrode's saline

The solution formulation developed by Tyrode [198] in 1910 accomplished two things simultaneously: (i) it introduced Mg^{2+} ions (0.53 mM) to saline solutions and (ii) it increased the HCO_3^- concentration to 11.9 mM (Table 3a). The HCO_3^- concentrations of the previous Ringer's and Locke's solutions were the same, i.e. 2.38 mM. This author was unable to find any studies which used Tyrode's saline as a medium for the biomimetic synthesis of calcium phosphates.

5.2. Krebs–Henseleit buffer (KHB)

The physiological saline formulation published in 1932 by Krebs and Henseleit [199] increased the HCO_3^- concentration to 25 mM, the Mg^{2+} concentration to 1.25 mM, the Ca^{2+} concentration to 2.52 mM and the K^+ concentration to 5.88 mM, and, more importantly, added phosphate ions at a concentration of 1.18 mM and SO_4^{2-} ions at a concentration of 1.25 mM (Table 3a). The composition of this physiological saline, KHB, represented an approximation to the composition of human blood plasma. KHB seems to be one of the earliest metastable, supersaturated (with respect to the precipitation of carbonated and ion-substituted apatitic CaP) calcium phosphate solutions. KHB has a Ca/P molar ratio of 2.136. It was not surprising at all to see precise numerical tables for the composition of human blood plasma and serum later (in 1950) contributed by Krebs [9], indicative of the immense knowledge Krebs had accrued in this field. The concentrations of the inorganic constituents and those of the amino acids of human blood plasma were tabulated by Krebs [9] in a review article.

KHB is commercially available today in powder form, which requires the further, separate additions of both $CaCl_2{\cdot}2H_2O$ and $NaHCO_3$ salts during the solution preparation using water. Krebs-Henseleit buffer should not be confused with Krebs–Ringer bicarbonate buffer, also available from a number of commercial vendors, which has reduced concentrations of Mg^{2+} and HCO_3^- and is Ca-free. Solutions such as KHB are also known as balanced salt solutions, and are used by medical researchers in tissue culture studies to maintain the tissue medium within the physiological pH range and supply essential inorganic ions. Most of the time, such balanced salt solutions are supplemented with glucose to provide energy to the cultured tissues. This is why the majority of media shown in Tables 3a and 3b were originally developed to have 1–2 g l^{-1} glucose in their formulations [166].

Unfortunately, finding any studies which used KHB as the CaP synthesis/biomineralization medium is difficult, if not impossible. This may point to a gap present between medical research and materials science research.

5.3. Earle's balanced salt solution (EBSS)

The isotonic (i.e., having the same osmotic pressure as blood) saline solution published in 1943 by Earle [200] reduced the K^+, Mg^{2+}, Ca^{2+}, HPO_4^{2-}, Cl^- and SO_4^{2-} concentrations of the KHB solution and slightly increased the HCO_3^- concentration to 26.2 mM (from 25 mM of KHB). The reductions achieved in K^+, HPO_4^{2-}, Cl^- and SO_4^{2-} and the slight increase in HCO_3^- concentration rendered the composition of the EBSS much closer to that of ECF (Tables 1 and 3a). Nevertheless, the significant reductions in the Ca^{2+} (from 2.52 to 1.8 mM) and Mg^{2+} (from 1.25 to 0.83 mM) concentrations of EBSS, with respect to those of KHB, may be deemed as steps taken backwards to the Tyrode solution. Apparently, Earle did not report any intention, in his studies, of developing a solution to mimic the ion concentrations of ECF, even though he and his co-workers could easily have done so [201,202]. A number of different modifications or derivatives of the original EBSS formulation are also available today from commercial vendors of balanced salt solutions.

Termine and Eanes [203] used EBSS as the physiological medium for the biomimetic synthesis of calcium phosphate nanoparticles at physiological pH (7.4) and temperature (37 °C). This

[1] Ringer's solution tablets, ¼ strength. Available from: http://www.sigmaaldrich.com.

study is one of the most important works (since it contains TEM photomicrographs of synthesized CaPs) on the biomimetic synthesis of CaPs using a physiological solution. Most physiological fluids, with ion concentrations more or less similar to that of ECF, have the potential to form carbonated and ion-substituted apatitic or amorphous calcium phosphate *de novo* in the absence of any nucleating or inhibitory agent. Termine and Eanes [203] buffered the EBSS using 25 mM HEPES (2-(4-(2-hydroxyethyl)-1-piperazinyl)ethane sulphonic acid, $C_8H_{18}N_2O_4S$) at pH 7.4 (and 37 °C), then added the salts of $CaCl_2$ and Na_2HPO_4 at the level of 2.1 mM^2, in terms of Ca × P molar product, to initiate the synthesis. It should be noted that the Ca × P molar product of the original EBSS formulation was only 1.87 mM^2 (Table 3a). Termine and Eanes [203] reported that they formed quite small amounts (only 3–5% of the total calcium and phosphate ions being actually precipitated) of ACP spherules with diameters in the vicinity of 100 nm within the first 24 h of aging their solution at 37 °C. In a follow-up study published in 1976, Eanes [204], by pursuing the biomimetic synthesis using a HEPES-buffered EBSS-like medium, further elaborated on the experimental conditions which cause the transformation of ACP spherules into needle-like cryptocrystalline Ap-CaP crystals. The high-resolution TEM photomicrographs provided in both studies [203,204] should guide CaP research interested in the biomimetic synthesis of calcium phosphates in the future. The hydrothermal transformation (or maturation) of ACP into cryptocrystalline Ap-CaP is beyond the scope of this review; a review of this topic may be found elsewhere [84].

Unfortunately, work using EBSS as the medium to synthesize calcium phosphates is not voluminous. Tuck et al. [205] investigated the dissolution and hydration of silicon-stabilized α-tricalcium phosphate (α-TCP, α-$Ca_3(PO_4)_2$) samples in a commercially available EBSS solution. Since α-TCP hydrolyzes readily in deionized water or 0.9% NaCl, 0.5–3.5% Na_2HPO_4 or SBF solutions, it would also hydrolyze and dissolve in the chosen EBSS solution by reprecipitating into Ca-deficient, ion-substituted and carbonated Ap-CaP [206]. Shadanbaz et al. [207] only used EBSS as a corrosion test medium for their uncoated or CaP-coated Mg metal samples and did not provide any chemical analysis results for the CaPs formed on the sample surfaces upon immersion in the EBSS.

5.4. Hanks' balanced salt solution (HBSS)

Hanks' balanced salt solution (HBSS) [208,209], in comparison to KHB, reduced the HCO_3^- concentration sharply to 4.065 mM, reduced the Ca^{2+} concentration to 1.26 mM, while significantly increasing that of Cl^- to 144.8 mM. Readers should be alert to the fact that commercial vendors offer dozens of variations of the HBSS solution, which may even come in calcium-, magnesium- or bicarbonate-free forms, while keeping the same name. The original HBSS solution was also not HEPES-buffered in contrast to what is occasionally sold nowadays. One may thus mention today of an inflation of physiological salines available through commercial vendors, and this may also make it quite difficult to compare the results obtained in various studies performed with different derivatives of the HBSS solution and its derivatives in the future.

If one compares, in chronological order, the four physiological salines reviewed so far in this chapter, namely Tyrode (1910), KHB (1932), EBSS (1943) and HBSS (1949), it can be seen that the Ca/P molar ratios of these solutions drop from 5.45 (Tyrode) to 2.136 (KHB) to 1.731 (EBSS) and finally to 1.615 (HBSS). Hanks and Wallace [208] article did not mention any aim of developing a saline that would mimic the composition of the inorganic ion concentrations of blood plasma.

The literature suffers from controversy about the actual HCO_3^- concentration of HBSS and, as exemplified in the literature review below, almost all researchers assumed its HCO_3^- concentration as 4.2 mM when preparing their own HBSS solutions. In order to resolve this issue, it is necessary here to quote directly from their 1949 article how Hanks and Wallace originally described the $NaHCO_3$ addition to their solution [208]: "The solution was autoclaved in 20 cc amounts in screw cap Pyrex bottles. One half cubic centimeter of autoclaved 1.4% (isotonic) $NaHCO_3$ was added to each bottle and the solution stored in the refrigerator for CO_2 equilibration to pH 7.6 before final tightening of the caps."

The above-mentioned 1.4% $NaHCO_3$ solution contains 14 mg of $NaHCO_3$ in each milliliter, which corresponds to 7 mg in half of a cubic centimeter of the solution. Upon adding 0.5 ml of $NaHCO_3$ solution to 20 ml of $NaHCO_3$-free HBSS, the total volume of the solution becomes 20.5 ml. The 7 mg of $NaHCO_3$ in the 20.5 ml corresponds to 0.342 g l^{-1}, which is then equal to 4.065 mM HCO_3^-. The HCO_3^- concentration of HBSS in Table 3a is indicated as 4.065 mM, since only the original articles of the inventors/developers of such solutions or media are reviewed herein. Quite a lot of research articles published, which refer to HBSS-like solutions with a bicarbonate concentration of 4.2 mM (or 0.35 g l^{-1} of $NaHCO_3$ = 4.166 mM).

The use of HBSS (in conjunction with calcium phosphates) started in 1990, with the study of Huigen et al. [210], who used HBSS as an incubation medium for testing the adsorption–desorption of diphosphonate–Tc(Sn) complexes on β-TCP samples at 37 °C. Kummer and Jaffe [211] simultaneously compared 0.9% NaCl (154 mM NaCl) solution, Ringer's solution and HBSS in monitoring the dissolution–reprecipitation phenomena on plasma-sprayed (mostly with Ap-CaP) Ti–6Al–4V and Co–Cr–Mo alloy samples. HBSS was usually used as a testing/incubation medium for CaP-coated or chemically treated metallic implant materials [212–239], and most of these studies regarded HBSS as an alternative to the EBSS (Earle's balanced salt solution) or SBF (simulated/synthetic body fluid) solutions in spite of its significant insufficiency in mimicking the composition of ECF. Just like Ringer's saline, the HBSS solution was also used to perform stability and dissolution tests on CaP bioceramics (brushite, apatite and TCP), CaP cements based on α-TCP or tetracalcium phosphate ($Ca_4(PO_4)_2O$) and bioglasses at room temperature or 37 °C [240–263]. This review could not find any research that used HBSS as a solution to synthesize calcium phosphate powders.

5.5. Eagle's minimum essential medium (Eagle's MEM)

The first physiological solution containing amino acids, vitamins, glucose and inorganic ions simultaneously (in contrast to amino acid-free Ringer's, Tyrode's, KHB, EBSS or HBSS solutions) was suggested in 1959 by Eagle [264–266]. Eagle called this saline as the minimum essential medium and since then it is abbreviated as MEM [264]. Eagle's MEM formulation contained 13 L-amino acids (i.e. arginine, cystine, glutamine, histidine, isoleucine, leucine, lysine, methionine, phenylalanine, threonine, tryptophan, tyrosine and valine), eight vitamins (i.e. choline, folic acid, inositol, nicotinamide, pantothenate, pyridoxal, riboflavin and thiamine) and glucose. The amino acids, vitamins and glucose were added to keep the cells alive in this physiological saline solution.

The inorganic ions compartment of Eagle's MEM solution is shown in Table 3a. The development of such solutions or media provided researchers with the ability to perform cell culture analyses in almost every laboratory around the globe. The inorganic electrolyte compartment of Eagle's MEM tried to remedy the deficiencies presented by the HBSS formulation, by increasing the HCO_3^-, Mg^{2+}, Ca^{2+}, and HPO_4^{2-} concentrations to the levels of the blood plasma, while slightly decreasing the K^+ and Cl^- concentrations to the level of EBSS and blood plasma. In a sense, as seen in Table 3a, Eagle's MEM solution resembled EBSS.

The essence of the matter here is that any researcher can immerse or soak any synthetic biometal, bioceramic or biopolymer

sample in any saline solution available for testing their physical properties [174–196,212–263] but, in order to keep the cells alive, spreading, proliferating or differentiating on the surfaces of the immersed biomaterials, all of the ion concentrations in the immersion medium must be quite close to the composition of ECF [267]. Alpha-MEM is a commercially available enriched cell culture medium version of Eagle's original MEM solution that contains 21 amino acids and a number of additional vitamins.[2]

5.6. Dulbecco's modified Eagle's medium (DMEM)

Dulbecco's modified Eagle medium [268,269] is another cell culture solution, with a much higher HCO_3^- concentration (44.05 mM) than Eagle's original MEM formulation, as shown in Table 3a. DMEM media are available today from commercial vendors (in either liquid or powder form) and there are quite a number of variants of DMEM available, mainly in forms containing high, low or no glucose at all, with or without glutamine, with or without Na-pyruvate, with or without phenol red, and with or without HEPES.[2] As a consequence, it may not be appropriate to assume that the findings of one study which used a specific DMEM solution containing glucose, glutamine, Na-pyruvate and HEPES will be the same as or similar to the findings of another study utilizing another DMEM solution without one or more of these additives. Therefore, it is important in any publication to include the catalog number assigned by the manufacturer to the specific DMEM used. Calcium phosphate researchers usually use one of the above media (i.e. α-MEM or DMEM) when they need to perform in vitro cell culture tests on their synthetic biomaterial samples.

The solution named ACP in Table 3a is a completely inorganic solution, free of amino acids, vitamins, glucose and HEPES, that was developed recently [270]. The ACP solution is somewhat similar to the inorganic ion compartment of a DMEM solution. The ACP solution has its Ca^{2+} concentration increased to 2.262 mM so that, without changing the DMEM's HPO_4^{2-} concentration (i.e. 0.905 mM), the Ca/P molar ratio of the new solution is adjusted to 2.50, with a Ca × P molar product of 2.047 mM^2 and an ionic strength of 0.141 M.

This Ca × P molar product, sometimes called ionic product (IP), can be related, by Eq. (2), to the relative supersaturation (σ) that the synthesis solution possesses, where K_s° is the solubility product of the solid phase separating from the mother liquor and v is the total number of ions in its chemical formula [271]. Using such a simplified formula as

$$\sigma = (\mathrm{IP}/K_s^\circ)^{1/v} - 1 \quad (2)$$

could be risky, especially when the solid separating from the mother liquor is non-stoichiometric and ion-substituted, and when its solubility product (K_s°) as well as its chemical formula (therefore v) have not yet been determined experimentally. The literature using such simple formulas, which assume that the precipitating phase is stoichiometric HA ($Ca_{10}(PO_4)_6(OH)_2$), is abundant. Moreover, IP and K_s° values imply that each ion is free and behaves individually, with no interactions whatsoever with other ions present in the solution. It is theoretically impossible to precipitate stoichiometric HA if the mother liquor is a physiological solution or a biomineralization medium containing several biologically relevant ions simultaneously. The solution of Termine and Eanes [203], mentioned in Section 5.3 above, was 25 mM HEPES-buffered, had a Ca × P molar product of 2.1 mM^2 and needed subsequent $CaCl_2$ and Na_2HPO_4 additions to precipitate small quantities of ACP nanospherules. The ACP solution with a Ca × P molar product (2.047 mM^2) similar to that of Termine and Eanes [203], on the other hand, needs no salt additions to start the synthesis of ACP, and its pH buffering ability comes from the use of 44.05 mM HCO_3^-, identical to that of DMEM solutions. This precipitate-free (to the naked eye) solution has the ability of in situ precipitating X-ray-amorphous, monodisperse nanospherules (105–170 nm diameter) of ACP when simply heated and stirred at 65 °C for 1 h (Fig. 2a). The synthesis of X-ray-amorphous CaP precipitates in the ACP solution at 37 °C takes a little over 1 h and the ACP solution is prepared by dissolving NaCl, KCl, $MgCl_2{\cdot}6H_2O$, $CaCl_2{\cdot}2H_2O$, $NaH_2PO_4{\cdot}H_2O$ and $NaHCO_3$ salts at room temperature, in the order given, in pre-boiled deionized water to a total volume of 1 l (Table 3b) [270]. Fig. 2b depicts the X-ray diffraction (XRD) and Fourier transform infrared spectroscopy (FTIR) data of the hydrated ACP spherules, which were also found to be magnesium- and carbonate-doped. These Mg-stabilized ACP nanospherules synthesized using the ACP solution (Tables 3a and 3b) did not transform into cryptocrystalline Ap-CaP even after 1 week of soaking in their mother liquors at 37 °C, in contrast to what was reported by Greenfield et al. [272]. The use of EBSS by Termine and Eanes [203] and the ACP solution of Table 3a [270] are examples of the synthesis of calcium phosphates in physiological solutions or media.

DMEM solutions, which contain amino acids and vitamins, were tested as media of mineralization for a number of synthetic biomaterials. Cisar et al. [273] increased the calcium and phosphate ion concentration in their DMEM solution to 10 mM (i.e. a 5.5X increase in the Ca^{2+} concentration of the original DMEM) by adding calcium chloride and sodium phosphate salts, then immersed apatite powders in this solution for up to about 1 month (at 37 °C); they reported the formation of nanospheres of CaP (confirmed by their infrared spectroscopy data). More recently, Rao et al. [274], following the previously published procedure of Cisar et al. [273], increased the calcium ion concentration of DMEM up to 10 mM; soaked collagen–chitosan hybrids (hydrogels) in the resultant solutions and only reported calcium deposition. Rao et al. [274] study did not report any infrared or XRD data to identify the CaP phase(s) forming on the hydrogels.

Gomes et al. [275], Mandel and Tas [276] and Lee et al. [277] suggested using DMEM as an alternative to the SBF solutions in the biomimetic processing of CaP specimens at 37 °C and pH 7.4. Lutisanova et al. [278,279] soaked bioglass and glass–ceramics in DMEM solution at 37 °C, followed by the microscopic examination of the spherulites (or globules) forming on the sample surfaces. By only reporting energy-dispersive X-ray spectroscopy (EDXS) data, these studies [277–279] proved that the DMEM solution used was able to cover the bioglass, glass–ceramic or CaP sample surfaces with spherulites of a CaP phase. Nevertheless, none of these reports [277–279] provided any XRD data to ascertain whether the CaP formed on the sample surfaces upon immersion in DMEM was amorphous, cryptocrystalline (i.e. yielding poor-crystallinity XRD patterns incapable of resolving the crystalline HA's quartet of peaks, namely (211), (112), (300) and (202) reflections, over the Cu K_α radiation 2θ range of 30–35°) or crystalline, as well as whether the CaP phase contained any octacalcium phosphate and/or brushite or not. Declercq et al. [280], on the other hand, had previously given quite a proficient example of how to use experimental XRD and FTIR techniques to monitor the extent of biomineralization (or calcification) on rat osteoblast cells (without any soaked biomaterial) kept in a cell culture medium.

Immersion tests which used HEPES-free DMEM solutions containing phenol red instead of SBF have been performed only on Ti6Al4V alloy substrates, not on pure Ti samples. Faure et al. [281] soaked NaOH-treated (10 M NaOH solution, 60 °C for 24 h) Ti6Al4V substrates in a DMEM solution (free of HEPES buffer, but containing phenol red and Na-pyruvate) at 37 °C, and reported, using XRD data, that well-crystallized Ap-CaP formed on the substrates. However, the low-magnification SEM photomicrographs provided by Faure

[2] Available from different commercial vendors specializing in the production of cell culture media. The author abstains from naming any one specific vendor here.

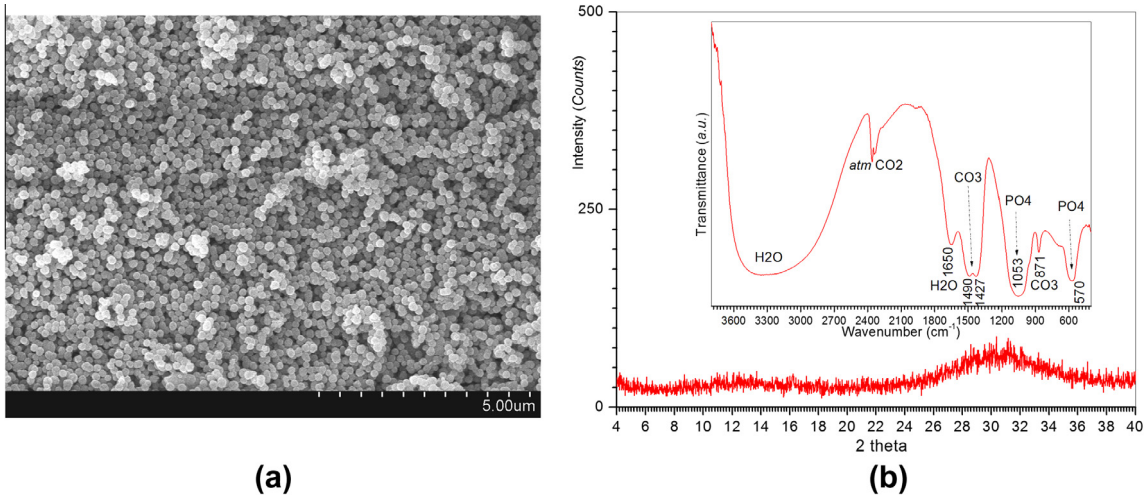

Fig. 2. (a) SEM and (b) XRD–FTIR data of X-ray amorphous CaP powders synthesized in solution ACP of Tables 3a and 3b.

et al. [281] made the detection and differentiation of the morphology of the formed Ap-CaP particles from the texture of the underlying NaOH-treatment layer somewhat difficult. Benhayoune et al. [282,283] soaked Ti6Al4V samples coated with an electrodeposited CaP layer in a DMEM solution (again HEPES-free, but containing Na-pyruvate and phenol red) at 37 °C and observed the formation of new Ap-CaP nuclei on the sample surfaces. HEPES-buffered and phenol red-free DMEM solutions have not yet been used to specifically test pure titanium surfaces.

Fetal bovine serum (FBS) is usually added to DMEM solutions when performing cell culture studies. FBS itself contains amino acids, glucose, proteins, polypeptides and hormones. Liu et al. [284] reported that a HEPES-free physiological medium, namely RPMI-1640 (similar in composition to DMEM solutions but with a significantly lower HCO_3^- concentration of 23.81 mM), was able to form micron-size cryptocrystalline Ap-CaP particles (but not ACP) when heated at 37 °C for 24 h. However, upon adding 10 vol.% FBS to RPMI-1640, the CaP precipitates forming were less than 100 nm in diameter and X-ray-amorphous. The significance of the data of Liu et al. [284] is that it shows the cryptocrystalline Ap-CaP forming tendency of a cell culture medium that is HEPES-free, low in HCO_3^- concentration (with respect to DMEM) and containing amino acids, vitamins and glucose, essentially similar to the DMEM solutions previous research used, in coating Ti alloy substrates [281–283].

In any discussion related to the DMEM solutions, one should note, using the findings of Chaudhary et al. [285], that bone marrow stromal cells cultured in a DMEM or α-MEM solution together with BMP-7 (a bone morphogenetic protein) in situ produces Ap-CaP. This review found that DMEM (or α-MEM), a medium of choice in cell culture studies, has a strong potential for the biomimetic synthesis of calcium phosphates at 37 °C and pH 7.4. This potential of DMEM (or α-MEM) has not yet been fully exploited.

5.7. CaP synthesis in solutions mimicking the composition of ECF

It was reported in 1945 by Greenwald [286] that the solubility of calcium phosphate is measurably increased by the presence of carbonate in its lattice. This explains why non-stoichiometric yet apatitic CaP bioceramics, which undergo resorption under the action of osteoclast cells, are usually carbonated apatites but not carbonate-free, stoichiometric HA [287–289]. The carbonate present as a component could either be exchanged with phosphate (or hydroxyl) on already formed Ap-CaP crystals or co-precipitated with Ca^{2+} and HPO_4^{2-} from carbonated metastable solutions at or close to the physiological pH of 7.4 [14,44,72]. Gron et al. [287] provided experimental evidence that the solid precipitates formed from metastable aqueous solutions of Ca^{2+} and HPO_4^{2-} (with ionic strengths, i.e. 0.15–0.16 M, close to that of ECF) contained carbonate in proportion to the concentration of HCO_3^- in the solution. It has also been known since 1938 that the solubility of biological or synthetic HA is higher in blood serum (having a 27 mM carbonate ion concentration) than in CO_2-free aqueous solutions of comparable ionic strength [290]. In the light of the above early knowledge, it is not easy to explain the reasons for the choice of carbonate-deficient Ringer's saline (2.38 mM HCO_3^-) or Hanks' (4.065 mM) solutions in testing the dissolution/stability of HA samples [174–196,212–263].

Bachra et al. [291–293] published, in 1962 and 1963, the synthesis of calcium phosphates at 37 °C and pH 7.3 in solutions partially mimicking (i.e. Mg-free) the inorganic ion concentrations of ECF. Their solutions contained 145 mM Na^+, 133 mM Cl^-, 5 mM K^+, 3.75 mM Ca^{2+}, 1.67 mM P and 22 mM HCO_3^-, with an ionic strength of 0.16 M. These solutions were aged statically (i.e. without stirring) in glass flasks at 37 °C for 5–72 h. They noted that the amount of precipitates collected rarely exceeded 10 mg. Bachra et al. [291–293] also repeated the same experiments with solutions containing 110 mM HCO_3^-. ACP was obtained in all of these high [HCO_3^-] experiments, and the ACP precipitates transformed into cryptocrystalline Ap-CaP when they were kept in contact with their mother solution for several days at 37 °C. This transformation to cryptocrystalline Ap-CaP was probably due to the absence of Mg^{2+} ions in the synthesis solutions. Bachra et al. [291–293] made the important experimental observation that by raising the carbonate level sufficiently (i.e. to 110 mM) they were able to slow down the ACP-to-cryptocrystalline apatite transformation and obtain stable amorphous precipitates. In their follow-up study in 1965, Bachra et al. [294] reported the influence of the presence of Mg^{2+} in such solutions at concentrations of 1, 3 and 10 mM. Bachra et al. [294] also observed a significant decrease in the crystallinity of precipitates upon adding 1 mM Mg^{2+} to the biomimetic solutions, and reported the formation of only ACP precipitates when they increased the concentration of Mg^{2+} to 3 mM and above, while studying the HCO_3^- concentrations of 22 and 110 mM at the increased Mg levels. These were quite important early studies conducted with solutions mimicking the ECF at 37 °C and pH 7.4. Posner et al. [87,295,296] did not perform their

ACP syntheses in solutions simultaneously containing Na^+, Mg^{2+}, K^+, Cl^- and HCO_3^- at concentration levels similar to those of bone tissue fluids.

Besides the above significant contributions to the calcium phosphate field, Bachra and his co-workers had published two interesting articles in 1959 on the mineralization of collagen fibrils [297,298]. In comparison to the more recent collagen fiber mineralization research [98–144] cited in above in Section 3, Bachra et al. [297,298] used a calcification solution containing Na^+, K^+, Ca^{2+}, Mg^{2+}, HPO_4^{2-}, Cl^- and HCO_3^- (at 22 mM) which tried to mimic the bone tissue fluid (or ECF). They studied the mineralization of collagen fibers (complete with post-treatment chemical analyses) in this solution at 37 °C and pH 7.3, which was previously developed by Goldenberg and Sobel [299] in 1952. Bachra et al. [297,298] reported that the rat-tail tendon and skin acid-soluble collagen fibrils they tested mineralized only poorly, and that the first nuclei forming on collagen could be ACP rather than apatite.

More recently, Nudelman et al. [140] observed, using a powerful transmission electron microscope, the initial formation of ACP on collagen fibrils soaked in polyaspartic acid-containing aqueous but HCO_3^- and Mg-free calcification solutions. Apparently, with today's powerful electron microscopes and their chemical and structural analysis attachments (such as wavelength-dispersive X-ray spectroscopy, EDXS and electron-backscatter diffraction), it would be timely to study the mineralization of collagen fibers soaked at 37 °C and pH 7.4 in metastable calcium phosphate solutions (free of any organic molecules), which simply mimic all the inorganic ion concentrations of the ECF. The resulting phase of ACP, instead of apatite, should not be a surprise in more recent research, since it was reported as long as 54 years ago, though was apparently overlooked. To summarize, the contributions of Bachra et al. [291–294,297,298] to both collagen–CaP biomimetic hybrid processing (1959) and biomimetic CaP synthesis (1962 and 1963) are still of significance today.

Okazaki et al.'s 1982 contribution [300] brought an entirely different physiological saline to the biomimetic CaP processing field, i.e. the dialysate solutions that are produced commercially[3] for the artificial kidney systems of dialysis patients. Okazaki et al. [300] prepared metastable physiological solutions based on artificial kidney dialysates and the reported solutions of pH 7.3 closely mimicked the Na^+, K^+, Ca^{2+}, Mg^{2+}, Cl^-, HCO_3^- and HPO_4^{2-} concentrations of ECF, without any deficiency in the concentrations of the ions. They used these solutions as an incubation medium (at 37 °C for 1 month) for the carbonated apatite powder samples (250 mg of powder in 100 ml of solution) that they synthesized, and compared the performance of the dialysate solutions with that of distilled water. Okazaki et al. [300] observed and reported a slight yet detectable decrease in the crystallinity (measured by XRD) of carbonated apatite samples soaked at 37 °C in the metastable dialysate solutions for 1 month vs. those soaked in distilled water.

This section may be concluded by the words of Termine et al. [301], published in 1980: "when the *de novo* calcium phosphate synthesis was performed at 37 °C and pH 7.4 in synthetic extracellular fluids (such as EBSS), apatitic crystal formation proceeds from an amorphous calcium phosphate (ACP) precursor at ionic Ca^{2+} and HPO_4^{2-} concentrations close to those found in physiological fluids".

5.8. CaP processing via simulated body fluids

Kokubo et al. formulated the simulated body fluid (SBF) solution in 1987 [302]. This early version did not contain any SO_4^{2-} ions and was buffered using Tris–HCl pair (50 mM Tris) at the pH 7.25 (36.5 °C). The solution was developed as a medium to test the in situ three-point bending strength of glass–ceramics and was prepared by dissolving NaCl, $NaHCO_3$, KCl, $K_2HPO_4{\cdot}3H_2O$, $MgCl_2{\cdot}6H_2O$ and $CaCl_2$ in water. Tris is the abbreviation for the organic chemical tris-hydroxymethyl-aminomethane, $(HOCH_2)_3CNH_2$, which is not present in human metabolism. Kokubo et al. then added Na_2SO_4 to the preparation recipe without changing the other salts, and obtained the formulation labeled SBF in Table 3a [20]. The Na_2SO_4-added SBF solution was buffered at pH 7.4 instead of 7.25 [302], again by using 50 mM Tris.

Interestingly, the HCO_3^- and Cl^- concentrations of the SBF formulation, of 4.2 (too low) and 148 (too high) mM, respectively [20], were identical with those of HBSS [208]. Kokubo's SBF solution deposited on the substrates (metallic, ceramic, glass or polymer), immersed in it for up to four weeks, poorly crystallized (cryptocrystalline) apatitic calcium phosphate, but not amorphous calcium phosphate (ACP). Kokubo group has published prolifically, since 1990, over 256 articles [303] on their SBF solution. As a result, the 50 mM Tris–HCl-buffered SBF solution with 4.2 mM HCO_3^- and 148 mM Cl^- is currently used in a significant number of research studies as a tool to predict the so-called in vivo bone bioactivity of synthetic biomaterials [304,305]. The SBF solution does not seem to be the most suitable in vitro test medium for the evaluation of in vivo bone bioactivity; for reasons explained by Pan et al. [306] and by Bohner and Lemaitre [307].

Tas and Bayraktar [47–49] noted that if one only changes the salt of $K_2HPO_4{\cdot}3H_2O$ used in preparing the solution of the Kokubo formulation to Na_2HPO_4 or $Na_2HPO_4{\cdot}2H_2O$, the deficiency in HCO_3^- can be totally eliminated (with a final HCO_3^- of 27 mM being possible to attain in the new SBF solution) and the Cl^- concentration can be decreased to 125 mM (similar to those of the KHB [199] and EBSS [200] media) while still using the Tris–HCl pair for pH adjustment at 7.4 (37 °C). This 50 mM Tris-buffered solution with an HCO_3^- concentration of 27 mM is indicated in Tables 3a and 3b as SBF-T [47,48]. It is important to note here that the 40 ml of 1 M HCl added to the solution during preparation (Table 3b) is not reflected in the Cl^- concentrations of the SBF (148 mM) and SBF-T (125 mM) solutions, and that this inevitable HCl addition further increases the Cl^- concentration of the resultant solutions.

During the preparation of Tris-buffered SBF, the addition of Tris (6.06 g l^{-1} or 50 mM), in powder form, instantly increases the solution pH to slightly above 8.5, with an associated onset of solution turbidity. This value is then decreased to 7.4 at 37 °C by slowly adding small aliquots of 1 M HCl (which sum to about 40 ml) to finally obtain a solution that is transparent to the naked eye.

Do such freshly prepared transparent solutions still contain colloidal particles? Oyane et al. [308] found that colloidal particles with diameters in the vicinity of 1 nm were present in Tris–HCl-buffered SBF solutions by using dynamic light scattering. Yin and Stott [309] later elaborated on these experimental findings only by theoretical modeling of those colloidal particles (or Posner's clusters). One weakness of the model of Posner clusters [82,83,308–310], though, is that it does not account for the major dopants Mg^{2+}, Na^+ and HCO_3^-. It is quite difficult, if not impossible, to synthesize Mg^{2+}- and HCO_3^--free CaP in an SBF-T solution at 37 °C and pH 7.4. Tsuru et al. [311] studied the biomimetic apatite-inducing ability of silica gel samples immersed in 4.2 mM HCO_3^--containing Tris-buffered SBF solutions, of pH 7.25 [302], with different Ca^{2+} (2.5 and 3.7 mM) and HPO_4^{2-} (1.0 and 1.9 mM) concentrations, and found that increases in both concentrations accelerated the Ap-CaP nucleation rate from the precursor phase of amorphous CaP.

Upon heating 1 l of a freshly prepared Tris–HCl-buffered SBF solution at 37 °C in either a previously unused glass or polycarbonate plastic screw-cap bottle, small amounts of X-ray-amorphous CaP precipitates autogenously form and the amount of precipitates

[3] Kindaly I dialysate solution, Fuso Pharmaceutical Industries, Osaka, Japan (based on a private communication with Prof. Emeritus Masayuki Okazaki, Kyoto, Japan, July 2013).

observed increases with ageing time at that temperature [47–49]. This is due to the in situ aggregation and eventual sedimentation of those colloidal particles [308–310,312] that are initially present in the fresh SBF solution with increasing ageing time (at 37 °C), from several days to 1 month. Hashizume et al. [313] recently studied the autogenously formed precipitates of an SBF solution heated to 37 °C and reported that they are ACP at the moment they are formed, in support of the earlier report by Tas [48].

The buffer Tris present in the SBF solution has also been the subject of research since it is able to exert a strong influence on the extent of mineralization. Tris is known to form complexes with various cations, including Ca^{2+} and Mg^{2+} [314]. Marques et al. [244] and Serro and Saramago [315] reported that in Tris-buffered SBF solutions, unlike in those which were Tris-free, a fraction of the Ca^{2+} ions was bound into a stable solution complex and, consequently, fewer Ca^{2+} ions were available to deposit CaP on the immersed substrates. Moreover, a study by Rohanova et al. [316] stated that the Tris in their SBF solutions was causing increased dissolution of the surface constituents of bioglass and glass–ceramic samples soaked in it, thus leading to the premature crystallization of apatite on sample surfaces, tarnishing the reliability of in vitro bioactivity tests performed with such Tris-buffered SBF solutions. The amount of Tris used in preparing 1 l of an SBF solution is 6.06 g l^{-1} or 50 mM (see Table 3b). This is not a negligible amount, Tris becomes the third most abundant constituent of the SBF solution [20], after 142 mM Na^+ and 148 mM Cl^-. In response to the concerns about the presence of Tris in SBF, 5× [69,146,317–322] and 10× [68,323,324] SBF solutions (free of Tris) were developed, which also possessed an amplified ability to precipitate Ap-CaP on the surfaces of synthetic biomaterials immersed in them either at room temperature (RT) [68] or at 37 °C.

Kokubo group responded to the above-mentioned limitations of the SBF [20,302], which resembled the HBSS, by developing a revised-SBF solution and buffering it by using HEPES ($C_8H_{18}N_2O_4S$) in place of Tris. This new solution is labeled as SBF-H in Tables 3a and 3b, and it is able to match the ion concentrations of ECF perfectly [325–327]. However, the SBF-H solution used 11.93 g l^{-1} of HEPES in preparing the new solution, this amount again corresponding to 50 mM. It is important to note that when Termine and Eanes [203] used EBSS as a physiological medium for the biomimetic synthesis of CaPs, they buffered their solution by using 25 mM HEPES. Commercially available DMEM solutions are also buffered using only 25 mM HEPES [276]. Therefore, HEPES in the SBF-H solution (at 50 mM) is again the third most abundant constituent following 142 mM Na^+ and 103 mM Cl^-. In other words, in the SBF, SBF-T and SBF-H solutions the molar ratio of Tris/Ca^{2+} or HEPES/Ca^{2+} was set equal to 20, which is a significantly high number. Moreover, Tris and HEPES are not present at all in biological hard tissue fluids. The precipitates forming in SBF, SBF-T and SBF-H solutions (Tables 3a and 3b) at 37 °C and pH 7.4 were directly compared with one another by Jalota et al. [328]. Tris and HEPES are not readily or randomly interchangeable (with one another) buffers in physiological solutions or media in that their ability to keep the HCO_3^- in solution and to form complexes with biologically important ions such as Ca^{2+} and Mg^{2+} are different [314,329,330].

Attempts to use an SBF solution as the physiological medium to synthesize CaP powders in bulk quantities, at 37 °C and pH 7.4, have been relatively scarce, with the exception of the work of Tas and Bayraktar [47–49] and Landi et al. [50]. The Tris-buffered SBF used in these studies, with a HCO_3^- concentration of 27 mM, was the SBF-T solution shown in Tables 3a and 3b. SBF-T solutions produced amorphous CaP powders with an average particle diameter of 30 nm and were ion-substituted [48]. The SBF-synthesized ACP powders transformed into apatite when heated at 700–900 °C in air and they also possessed the unique ability of being stable to high-temperature calcinations performed at temperatures in excess of 1300 °C [48]. This is not a peculiar finding since the bones of cadavers recovered from high flame-temperature (1200 °C) and long-burning fires still showed apatite, but not β-TCP, in their XRD patterns [331,332]. Biological apatites are also of interest to forensic science researchers. Tas and Bayraktar [47] experimented with the use of urea in SBF-based biomimetic synthesis of CaPs. Dissolved urea partially decomposed in SBF-T solutions to produce HCO_3^- when the solution temperature reached 37 °C. In another study, Tas and Bayraktar [49] used urea together with its enzyme urease in SBF-T solutions at 37 °C to synthesize Ap-CaP nanoparticles. Enzyme urease catalyzed the decomposition of urea in the SBF-T solution at 37 °C. As a follow-up to the above, Landi et al. [50] independently tested the approach of using SBF-T solutions at 37 °C and pH 7.4 to produce CaP powders, and reported that the carbonated CaP powders (dried at 80 °C for 15 h) possessed a Brunauer–Emmett–Teller (BET) surface area of 160 m^2 g^{-1}. CaPs synthesized at 37 °C and pH 7.4 in a Tris–HCl-buffered SBF solution were also resistant to thermal decomposition into β-TCP (β-$Ca_3(PO_4)_2$) when heated above 1300 °C [48,50].

Ringer's lactated solution (RLS), also called as lactated Ringer injection, is currently used in hospitals in cases of trauma and resuscitation, as reviewed in Section 4. The composition and constituents of this solution are given in Tables 3a and 3b, respectively. It contains 28 mM Na-L-lactate, but does not contain any Tris or HEPES. There are two isomers of lactate (L and D) [173,333]. L-lactate is a part of normal human metabolism; it is oxidized to pyruvate by the enzyme lactate dehydrogenase and does not activate neutrophils. Neutrophils, being the predominant cells in pus, are recruited to the site of injury within minutes following trauma and are the trademark of acute inflammation [7]. In contrast, D-lactate is not part of normal human metabolism and is not oxidized by lactate dehydrogenase; therefore it accumulates and activates neutrophils. This is why RLS contains Na-L-lactate. This was also why Pasinli et al. [63] and Miller et al. [64] developed a new solution, which had the same inorganic ion concentrations as ECF, by using the Na-L-lactate and lactic acid pair to buffer the SBF-L solution (Tables 3a and 3b) at pH 7.4 and 37 °C. The SBF-L solution contains 22 mM Na-L-lactate, i.e. even less L-lactate than the 28 mM RLS [64,333]. Having physiological solutions or media with an inorganic ion composition mimicking that of ECF (which does not contain 50 mM Tris or 50 mM HEPES) is essential for biomimetic synthesis [334].

It might be appropriate in this section to briefly name and cite select examples of diverse materials the surfaces of which have been altered by using one or the other of SBF solutions given in Tables 3a and 3b: Teflon® [335], cotton [336], cellulose [337,338], CaP-containing calcium sulphate [142], whiskers of β-tricalcium phosphate (TCP), whiskers of biphasic HA/TCP or whiskers of HA [339,340], hydroxyethylmethacrylate (HEMA) [341,342], sodium silicate glasses [343], polyetheretherketone (PEEK) [344], quartz [345], silicon [346,347], chitosan [348], carboxylated polyphosphazene [349], polyethylene glycol [350], zirconium dioxide and aluminum oxide [351], polyethyleneterephthalate (PET) [352], dentin of human tooth [353], Fe_3O_4 (magnetite) [354], polyvinyl alcohol (PVA) [355], silicon carbide [356], titanium oxide [357,358], Ni–Ti alloy [359], silk [360], calcium silicate [361], magnesium silicate [362], calcium titanate [363], carbon nanotubes [364], 45S5 bioglass [365,366], magnesium alloys [367], pure magnesium [368], pectin [369], ethylene–vinyl alcohol (EVOH) with proteins [370] and chitosan/polyethylene glycol (PEG) hydrogels [371].

The SBF solutions proved useful in changing the physicochemical properties of their surfaces upon soaking at 37 °C and pH 7.4. Such alterations in the surface properties do not mean that the above materials (if they are not calcium phosphates at the beginning) then acquired some sort of bioactivity, biocompatibility

or non-cytotoxicity; rather, they gained a new surface simply through a process of carbonated, ion-substituted, non-stoichiometric and cryptocrystalline Ap-CaP deposition (only a few microns thick), which would probably be benign to the initial action of mammalian cells. The biological performance of the above materials can only be assessed after in vivo tests. Nevertheless, the only biocompatible and non-cytotoxic mineral the human body uses in non-pathologic formations is carbonated, ion-substituted and Ap-CaP.

Most of the above-mentioned SBF treatments were performed with the intention of coating the surface of a potential synthetic biomaterial with HA. Hydroxyapatite remains a popular term among many, although the hydroxyl ion deficiency in biological apatites and Ap-CaP synthesized in aqueous solutions have been well documented [14,73,74,76,88–90]. Biomimetic coating processes in SBF solutions are not able to coat stoichiometric HA on the surfaces of the immersed materials. Moreover, to obtain stoichiometric HA using any co-precipitation method at 37 °C and pH 7.4 is difficult, if not impossible. At pH 7.4 there would be no PO_4^{3-} ions in the aqueous solution; at this pH one can only have a mixture of HPO_4^{2-} (major) and $H_2PO_4^-$ (minor) ions [372]. The deviation from the stoichiometry reflects itself in the lattice distortions present in the precipitated apatites, even leading to the appearance of ACP [373]; and it is no surprise that Posner et al. [295] named such substances pseudoapatites as early as 1954. As Wheeler and Lewis [374] observed, mature cortical bovine bone, for instance, has only a paracrystalline (i.e. no long-range order) structure. The term hydroxyapatite, since it should only refer to the stoichiometric compound, is far from accurate in describing biological apatites having a paracrystalline, carbonated and non-stochiometric nature [372,374]. Wheeler and Lewis [374] also noted that only upon heating cortical bovine bones to 600–800 °C, the lattice stresses present in the pre-heated bones were relieved, its paracrystalline nature disappeared and the material became further hydroxylated, especially when firing the samples to the mentioned temperatures in a typically humid laboratory air atmosphere. The above observations matched the experimental FTIR data obtained during the incremental calcination of SBF-synthesized ACP powders well [48]. Wheeler and Lewis [374] pointed out a very important distinction between the XRD crystallite size and the TEM particle size (observed in the bright-field mode), and eloquently stated that the XRD crystallite size should always be less than the TEM particle size for biological apatites due to their paracrystalline nature. In the majority of articles the Scherrer equation [375] is used only on the (002) reflection obtained from the SBF-deposited Ap-CaP, and since the (211), (112), (300) and (202) quartet of reflections of the so-called "hydroxyapatite" cannot be resolved into separate peaks in the cryptocrystalline SBF-deposits or powders, the XRD crystallite size measurements reported tend to be inaccurate, and research has preferred to report the bright-field TEM particle sizes instead. Especially in the case of SBF-deposited pseudoapatites, the XRD crystallite size distribution should have been reported by using the multiple reflections-based Warren–Averbach and/or Williamson–Hall methods [81,376,377]. Rietveld analysis could also be satisfactorily used when the XRD data can present the above-mentioned quartet of reflections as individual peaks [378].

The literature on the SBF solutions is quite abundant, with some research reporting modified solutions by (i) separating calcium and phosphate ions into two separate solutions which are later mixed with one another or (ii) by eliminating some key constituents of the ECF, such as Mg^{2+} or HCO_3^-. Such solutions are not included in Tables 3a and 3b, as this review has focused only on single, homogeneous, optically transparent solutions, which try to mimic the ECF composition upon being buffered at a pH close to the physiological value. However, one special Tris–HCl-buffered (at pH 7.4 and RT) solution which does not contain Mg^{2+}, HCO_3^- and SO_4^{2-} ions can be given as an example to such solutions which are not included in Table 3a. This solution was published in articles in the late 1990s by Wen et al. [218,379,380] and was named supersaturated calcification solution (SCS). SCS contained 144.5 mM Cl^-, 136.8 mM Na^+, 4.64 mM K^+, 3.1 mM Ca^{2+} and 1.86 mM HPO_4^{2-}. It has higher Ca^{2+} and HPO_4^{2-} concentrations than physiological solutions or media, and its Ca/P molar ratio is adjusted to a lower value (1.667). It is possible to prepare this solution by using approximately 133.7 mM NaCl, 4.64 mM KCl, 3.1 mM $CaCl_2{\cdot}2H_2O$ and 1.86 mM Na_2HPO_4. Wen et al. [379,380] studied this solution at 37 °C as a function of the immersion time of Ti and/or Ti6Al4V substrates, and reported that the CaP deposition consisted of three stages: (i) precipitation of ACP within the first 2 h; (ii) transformation of ACP into apatite between 4 and 6 h; and (iii) the subsequent crystallization of OCP (octacalcium phosphate, $Ca_8(HPO_4)_2(PO_4)_4{\cdot}5H_2O$) on the apatite layer. The in vitro solubility of OCP is higher than that of apatite [381] and, in most cases, this makes OCP a more favorable bone-substitute material than apatite [382]. The absence of Mg^{2+} and HCO_3^-, together with the slightly increased Ca^{2+} and HPO_4^{2-} concentrations, enabled this fast solution to deposit OCP in less than a day. Tas [383] found that the same SCS solution is quite effective in transforming single-phase brushite into single-phase OCP at 37 °C even without stirring.

The name SCS [218,380,381] should not be confused with the SPS (simulated physiologic solution) of Radin and Ducheyne [384], which is a Tris–HCl-buffered solution that did not have matching concentrations of the Ca^{2+}, Na^+ and Cl^- to those of the ECF. Speaking of name confusion(s), it may be of interest to note that the abbreviation SBF is also used by physiologists to denote either skeletal blood flow [385] or skin blood flow [386].

6. Role of proteins in calcium phosphate formation

The role of proteins in regulating and templating the calcium phosphate formation has been recently reviewed by Bleek and Taubert [28]. The current review, on the other hand, tabulated the ion concentrations of ECF. With such significant Ca^{2+}, Mg^{2+}, Na^+, K^+, Cl^-, HPO_4^{2-} and HCO_3^- concentrations in the ECF (Table 1), carbonated, ion-substituted and non-stoichiometric CaP would have precipitated all over the body, but fortunately it does not [22]. According to Rochette et al. [387], the serum glycoprotein fetuin-A, besides others, prevents pathological mineralization in ECF and in soft tissues, and such an inhibition was found to be related to the formation of calciprotein particles (of 25–150 nm in diameter). Rochette et al. [387] reported that those calciprotein particles consisted of amorphous CaP (ACP) and fetuin-A.

Poly(aspartic acid), (PAsp), like fetuin, has the potential of inhibiting CaP mineralization. Cantaert et al. [388] recently showed that ACP formed within 6 days in the presence of 50 μg ml^{-1} PAsp, in stark contrast to the formation of crystalline Ap-CaP (only after 3 h) in the absence of it, in experiments performed in a Tris–saline buffer solution at pH 7.4 (and 37 °C), having 4.5 mM $CaCl_2{\cdot}2H_2O$ and 2.1 mM $K_2HPO_4{\cdot}3H_2O$.

He et al. [389] revealed the role of dentin matrix protein (DMP1) in first binding calcium ions, secondly initiating the nucleation of amorphous CaP, and then expanding and coalescing into microscale apatitic CaP crystals elongated along the *c*-axis. If proteins were added to the physiological solutions or media reviewed here, it would be inevitable that the protein molecules would bind to the Ca^{2+} ions, possibly forming calciprotein nanoparticles in solution. Tsuji et al. [390], on the other hand, showed that, in the presence of DMP1 protein, ACP particles increased in size and the protein facilitated the reorganization of the internal structure of amorphous particles into ordered crystalline states, i.e. the direct

transformation of ACP to HA, thereby acting as a nucleus for precipitation of crystalline calcium phosphate. Tsuji et al. [390] also showed, with support from their TEM and XRD data, that ACP was the first phase to form in the absence of the protein.

The organic matrix of developing enamel consists of amelogenins, and Kwak et al. [391] found that native phosphorylated amelogenins can stabilize amorphous CaP for long periods of time (>1 day) in vitro. Kwak et al. [391] also noted that the recombinant non-phosphorylated amelogenin only transiently stabilized ACP and guided its transformation into ordered bundles of apatitic microcrystals of the enamel layer.

7. Synthetic urine and artificial saliva solutions

Urinary tract stones or calculi affect about 20% of the population and the mineral of those stones usually consists of single-phase or mixed calcium oxalate, calcium phosphate or uric acid. Struvite ($MgNH_4PO_4{\cdot}6H_2O$) stones, on the other hand, are more frequently seen in cats and dogs [392,393]. The understanding of the underlying mechanisms of pathological calcification processes may, therefore, be of interest to calcium phosphate research [394]. The composition of synthetic urine given in Table 3b corresponds to mean concentrations found in a 24 h period in normal human urine [395–397]. Research at the junction of urology and materials science, which uses synthetic urine formulations as the synthesis medium for calcium oxalates, struvite and calcium phosphates, seems to be quite rare [397].

Although human saliva is known to possess proteins, such as tyrosine-rich acidic peptide [398] or statherin [399], which inhibit calcium phosphate precipitation onto enamel surfaces, the artificial saliva formulation [400,401] given in Table 3a, which is supersaturated with respect to brushite formation, may prove helpful to calcium phosphate research. Brushite is one of the major phases of dental calculus [402]. Moreover, synthetic biomaterials that have a potential for use in the oral cavity need to be tested in artificial saliva solutions rather than, for instance, HEPES-buffered saline [403–405]. Leung and Darvell [406] provided 27 artificial saliva recipes in their comprehensive article.

Marques et al. [407] also reported a simulated saliva formulation, besides giving a number of useful formulations on how to prepare simulated synovial fluid, gastric fluid, intestinal and colonic fluids, lung fluid, vaginal fluid, semen, sweat and tears. The literature lacks any studies on the biomimetic synthesis of dental CaP materials in artificial saliva solutions, which could be crucial, especially for materials designed for root canal repair and pulp capping applications. Apparently, the artificial saliva solutions have only been used as post-synthesis test media for dental materials.

8. Summary and future directions

According to the present literature review, the use of physiological media or physiological salines, with compositions approximating that of ECF, in the biomimetic synthesis of calcium phosphate-based hard tissue substitutes at 37 °C and pH 7.4 have not gained much popularity, but quite competent examples have been uncovered and mentioned above in detail. The studies of Bachra et al. [291–294,297,298], Termine and Eanes [203], Eanes [204], Tas et al. [47–49] and Landi et al. [50] on the synthesis of CaPs at 37 °C and pH 7.4 directly in supersaturated or balanced salt solutions mimicking ECF were identified. These articles, published between 1959 and 2005, described the biomimetic synthesis of calcium phosphates, as well as the biomimetic processing of collagen–CaP hybrids or composites at the physiological pH and temperature. The Termine and Eanes [203] article, which described the formation of ACP nanospheres in an EBSS solution at 37 °C and pH 7.4, has received a relatively small number of citations since its publication in 1974.

There have been a couple of physiological solutions or media which have remained unnoticed for a number of decades, such as the Krebs–Henseleit buffer (formulated in 1932) [199] and Earle's balanced salt solution (1943) [200]. KHB and EBSS are physiological media that successfully mimic the composition of ECF. KHB and EBSS solutions set the HCO_3^- concentration in the supersaturated solutions at 25–26.2 mM, which is very close to that of ECF (i.e. 27 mM). Bachra's work from 1959 to 1965 showed that ACP precipitated either in supersaturated solutions with HCO_3^- concentrations close to that of ECF or when such solutions were used to mineralize collagen fibers. The work of Termine and Eanes in 1974 and 1976 showed again that ACP formed when EBSS at 37 °C and pH 7.4 was used as the synthesis medium instead of distilled water.

The KHB solution of 1932, with ion concentrations very similar to those of ECF, cannot produce "hydroxyapatite" when it is warmed up to 37 °C; it will only produce ACP. The same applies to EBSS, and to the SBF-T, SBH-H and SBF-L solutions described in this review. Mg^{2+} and HCO_3^- ions (which are well-known ACP stabilizers) and their concentrations available in KHB and EBSS, as well as in ECF, are responsible for the formation of ACP instead of HA in such solutions. In summary, any lactate-buffered (22 mM) aqueous solution having 95 mM NaCl, 5 mM KCl, 1.5 mM $MgCl_2{\cdot}6H_2O$, 25–27 mM $NaHCO_3$ and 2–2.5 mM $CaCl_2{\cdot}2H_2O$ would not precipitate stoichiometric or crystalline HA; rather, when 1 mM Na_2HPO_4 is introduced to this solution it will precipitate Mg- and HCO_3-stabilized nanospheres of ACP. The articles of Bachra et al. [291–294,297,298], Termine and Eanes [203] and Eanes [204] all showed that precipitates obtained from physiological solutions or media at pH 7.4 (at 37 °C) were ACP stable in their mother solutions, but not HA or cryptocrystalline Ap-CaP.

On the other hand, if one reacts a certain volume of an aqueous solution, free of any initial NaCl but having 1.67 mM $CaCl_2{\cdot}2H_2O$, with an equal volume of another solution which contains 1 mM Na_2HPO_4 (or K_2HPO_4) dissolved in it, where both solutions are strictly free of HCO_3^- and Mg^{2+} ions, one obtains cryptocrystalline or paracrystalline Ap-CaP phase exhibiting the weak and rather broad (002) reflection (at 25.89° 2θ, Cu K_α) in its XRD chart. During the first few minutes of mixing of these two solutions, ACP nanospheres are actually formed in the solution, but since the nanospheres are not stabilized by Mg^{2+} and HCO_3^-, they readily transform into Ap-CaP even before they are separated from their mother liquors [149–151,296].

The ossification in the fetus starts only by the end of the second month, close to the third month. Prior to the start of ossification in the fetus, there are only amniotic membranes in places of future bones. These soft and flexible membranes consist of stacked collagen fibrils, which are prone to the formation of layers of ACP on them. These start to transform into a cartilage-like tissue (as soft as the ears) at the turn of the third month, which then ossify in the following months under the action of the osteoblasts into bones until the day of delivery. An 8-week-old fetus is surrounded by the amniotic fluid within the amniotic sac. Although the electrolyte composition of the amniotic fluid is more or less similar to that of the ECF, its mean HCO_3^- concentration is 34 mM [408] and it contains 0.63 mM Mg^{2+} [409]. The relatively high bicarbonate ion concentration of 34 mM helps the formation of ACP on the membranes of the fetus. The fontanelles seen on the skull of a newborn baby, which are highly hydrated, soft and flexible substances like a piece of canvas [410,411], still possess a fraction of ACP.

The introduction of Hanks' balanced salt solution in 1949 [208], which had quite a low HCO_3^- concentration of only 4.065 mM and was developed for the stated purpose of preserving tissues under refrigeration at temperatures from 0° to 7°, may actually have helped the forthcoming research that was undertaken for the

purpose of synthesizing "hydroxyapatite" but not ACP. The review of the research shows that the well-known SBF solution [20] has a low HCO_3^- of 4.2 mM, and at this low concentration of the ACP stabilizer (i.e. HCO_3^-) Ap-CaP of poor crystallinity would readily precipitate on any surface by using a biomimetic coating process over a soaking period of up to 4 weeks [305]. Surely, upon soaking samples in the 4.2 mM HCO_3^- solution for 4 weeks, the initially precipitating ACP layers on samples would not be easily detectable, but Ap-CaP formed as a result of the maturation of ACP would be observed at the end of the long soaking period of 1 month [305]. This is possibly why a majority of research cites these observations as HA instead of Ap-CaP, even if the infrared data of such samples lack the OH^- stretching vibration at 3571 cm^{-1}. The literature indicates that the carbonate contents of such SBF-deposited Ap-CaP were only rarely determined [412].

Another interesting observation is related to testing the in vitro bioactivity of samples by immersion in a 4.2 mM HCO_3^- solution (SBF) first, complemented with the reporting of XRD charts showing the (002) crystallographic reflection of Ap-CaP and SEM images of SBF-precipitated Ap-CaP globules, followed by testing of samples by soaking them with various cells in a DMEM cell culture medium, which has a HCO_3^- concentration of 44.05 mM [413–415]. The use of two different solutions which differ 10.5-fold in their HCO_3^- concentrations presents a genuine difficulty in interpreting the results obtained from these two solutions for the same synthetic biomaterial in the same article. Some research seems to have overcome this difficulty by not providing results for samples recovered from the cell culture medium using XRD and FTIR, although Declercq et al. [280] have shown how to perform such analyses on cell culture samples. At this point, it is helpful to revisit the conclusions of Liu et al. [284], who stated that, especially in an FBS-supplemented cell culture medium, the CaPs formed will be less than 100 nm in diameter and X-ray-amorphous.

The concentration of the ACP stabilizer HCO_3^- is important, especially when both solutions contain the second stabilizer, Mg^{2+}. In order to prevent such complexities originating from the use of two different solutions for a given synthetic biomaterial, some researchers opted to use the same commercially available, sterile and amino acid-containing DMEM (or α-MEM) solution first as a physical stability/coherency test medium (in place of SBF) and then as the cell viability/proliferation/attachment test medium (see Section 5.6).

The current literature review on the use of physiological solutions, salines or media in calcium phosphate synthesis and processing suggests the following as future directions.

(1) The use of physiological solutions (such as EBSS, Bachra et al. solutions, ACP and SBF-T solutions of Table 3), in the place of distilled/deionized water, for CaP synthesis at 37 °C and pH 7.4 resulted in the production of ACP. Non-cytotoxic and biocompatible CaP biomaterials with large surface areas are needed especially in drug delivery applications of oncological and pharmaceutical research. The adsorption of blood proteins on a synthetic biomaterial requires a large BET surface area. Enriching the CaP-related research projects by collecting the BET surface area data seems to be crucial, especially when an assessment of the blood compatibility [416] of the biomaterial under question is required.

(2) Bulk synthesis of Mg- and CO_3-doped, monodisperse CaP nanospheres in physiological solutions or media, such as the Tris- and HEPES-free SBF-L and ACP solutions of Table 3, at 37 °C and pH 7.4 need to be further pursued. The synthesis of perfectly monodisperse, non-cytotoxic CaP nanospheres (which should not cross the blood–brain barrier (BBB) [417]) by using benign and biomimetic processes represents an interesting research field.

(3) The synthesis of submicron aragonite, calcite or vaterite ($CaCO_3$) particles in phosphate-free physiological solutions, such as KHB, EBSS, SBF-T, SBF-H, SBF-L or ACP (Table 3), has never been attempted. Such research may also shed light on the cause(s) of pathological $CaCO_3$ calcifications observed in humans [418–421].

(4) ACP has the ability of transforming into Ap-CaP (cryptocrystalline or paracrystalline), depending on its degree of stabilization by the biologically relevant ions Mg^{2+} and HCO_3^-. The same physiological solution (such as KHB, EBSS, ACP or SBF-L) in which the ACP nanospheres were formed can then be used to transform them into Ap-CaP in a controlled manner. Studies on the transformation kinetics of ACP in physiological solutions or media (at pH 7.4 and 37 °C) are seemingly scarce.

(5) The use of a common cell culture solution, such as DMEM or α-MEM, as a medium of CaP synthesis at 37 °C and pH 7.4 should be pursued. Moreover, the simultaneous adsorption of all of the amino acids present in a common cell culture medium onto the CaP nanoparticles nucleating within such solutions has never been studied.

(6) The addition of proteins to the physiological solutions reviewed here may present a fertile basic research field to learn more about the roles of Ca^{2+}, Mg^{2+} K^+, Na^+, HPO_4^{2-}, Cl^- and HCO_3^- ions coexisting at their physiological concentrations; literature on protein-containing KHB or EBSS solutions (which are commercially available) has been difficult to find. The influence of all blood proteins, such as albumins (ALB), immunoglobulin (IgG) antibodies, fibronectin (FNT), fibrinogen (FGN) and high molecular weight kininogen (HMK) [416], as well as osteopontin and bone morphogenetic proteins/growth factors, on biomimetic CaP synthesis (at 37 °C and pH 7.4) in physiological solutions or salines (Table 3) should be systematically studied with the aim of arriving at a comprehensive portrayal of the ECF–CaP duality or dichotomy.

(7) Nucleation studies (in relation to the synthesis of calcium phosphates, magnesium phosphates and calcium oxalates) to be performed in synthetic urine solutions at 37 °C may serve as a strong bridge between urology and biomaterials science.

(8) Biomimetic synthesis of novel dental materials (e.g. for pulp-capping or root canal infection cases) in artificial saliva solutions may also serve as a bridge between dentistry and biomaterials science.

Appendix Figures. with essential colour discrimination

Certain figures in this article, particularly Fig. 2, was difficult to interpret in black and white. The full color images can be found in the on-line version, at http://dx.doi.org/10.1016/j.actbio.2013.12.047.

References

[1] Gleick PH, editor. Water in crisis: a guide to the world's freshwater resources. Oxford: Oxford University Press; 1993. p. 13.
[2] Mann S. Biomineralization: principles and concepts in bioinorganic materials chemistry. Oxford: Oxford University Press; 2001.
[3] Lowenstam HA. Minerals formed by organisms. Science 1981;221:1126–31.
[4] Lowenstam HA, Weiner S. On biomineralization. Oxford: Oxford University Press; 1984.
[5] Barskov IS. Biomineralization and evolution. Coevolution of the mineral and biological worlds. In: Dobretsov N et al., editors. Biosphere origin and evolution. New York: Springer; 2008. p. 211.

[6] Taniguchi N. On the basic concept of nanotechnology, Proceedings of the international conference on production engineering Tokyo, Part 2. Tokyo: JSPE; 1974. p. 18–23.
[7] Ward JPT, Linden RWA. Physiology at a glance. Chichester: Wiley-Blackwell; 2008.
[8] Comparative Nutrition Society. The digestive system of vertebrates. Available from: http://www.cnsweb.org.
[9] Krebs HA. Chemical composition of blood plasma and serum. Annu Rev Biochem 1950;19:409–30.
[10] Saul JM. Did detoxification processes cause complex life to emerge? Lethaia 2009;42:179–84.
[11] W. Castro, Elemental analysis of biological matrices by laser ablation high resolution inductively coupled plasma mass spectrometry (LA-HR-ICP-MS) and high resolution inductively coupled plasma mass spectrometry (HR-ICP-MS) [PhD thesis]. Florida International University; 2008.
[12] LeGeros RZ, LeGeros JP. Phosphate minerals in human tissue. In: Nriagu JO, Moore PB, editors. Phosphate minerals. New York: Springer-Verlag; 1984. p. 351–95.
[13] Skinner HCW. Biominerals. Mineral Mag 2005;69:621–41.
[14] Glimcher MJ. Bone: nature of the calcium phosphate crystals and cellular, structural and physical chemical mechanisms in their formation. Rev Mineral Geochem 2006;64:223–82.
[15] Simkiss K. Bio-mineralization and detoxification. Calcif Tissue Res 1977;24:199–200.
[16] Leete E. Biomimetic synthesis of nicotine. J Chem Soc Chem Commun 1972;19:1091.
[17] Burke DE, DeMarkey CA, Cook JM, Le Quesne PW. Biomimetic synthesis of the bis-indole alkaloid macralstonine. J Chem Soc Chem Commun 1972;24:1346–7.
[18] Burke DE, Le Quesne PW. Biomimetic synthesis of the bis-indole alkaloid villalstonine. J Chem Soc Chem Commun 1972;11:478.
[19] Tabushi I, Imuta J. Biomimetic one-pot synthesis of nucleotide phosphates. Tetrahedron Lett 1982;23:5415–8.
[20] Abe Y, Kokubo T, Yamamuro T. Apatite coating on ceramics, metals and polymers using a biomimetic process. J Mater Sci Mater Med 1990;1:233–8.
[21] Mann S. Molecular tectonics in biomineralization and biomimetic materials chemistry. Nature 1993;365:499–505.
[22] Pasteris JD, Wopenka B, Valsami-Jones E. Bone and tooth mineralization: why apatite? Elements 2008;4:97–104.
[23] Sarikaya M, Aksay IA. Nacre: properties, crystallography, morphology, and formation. In: Sarikaya M, Aksay IA, editors. Design and processing of materials by biomimetics. Washington (DC): American Institute of Physics; 1993. p. 35–86.
[24] Sarikaya M. An introduction to biomimetics: a structural viewpoint. Microsc Res Techniq 1994;27:360–75.
[25] Dorozhkin SV. A detailed history of calcium orthophosphates from 1770s till 1950. Mater Sci Eng C 2013;33:3085–110.
[26] Dorozhkin SV. Bioceramics of calcium orthophosphates. Biomaterials 2010;31:1465–85.
[27] Boanini E, Gazzano M, Bigi A. Ionic substitutions in calcium phosphates synthesized at low temperature. Acta Biomater 2010;6:1882–94.
[28] Bleek K, Taubert A. New developments in polymer-controlled, bioinspired calcium phosphate mineralization from aqueous solution. Acta Biomater 2013;9:6283–321.
[29] Omelon SJ, Grynpas MD. Relationships between polyphosphate chemistry, biochemistry and apatite biomineralization. Chem Rev 2008;108:4694–715.
[30] Wang L, Nancollas GH. Pathways to biomineralization and biodemin eralization of calcium phosphates: the thermodynamic and kinetic controls. Dalton Trans 2009:2665–72.
[31] Coelfen H. Biomineralization: a crystal-clear view. Nat Mater 2010;9:960–1.
[32] Alves NM, Leonor IB, Azevedo HS, Reis RL, Mano JF. Designing biomaterials based on biomineralization of bone. J Mater Chem 2010; 20:2911–21.
[33] Boskey AL. Mineralization of bone and teeth. Elements 2007;3:385–91.
[34] Addadi L, Weiner S. Control and design principles in biological mineralization. Angew Chem Int Ed Engl 1992;31:153–69.
[35] Habibovic P, Barralet JE. Bioinorganics and biomaterials: bone repair. Acta Biomater 2011;7:3013–26.
[36] Bose S, Tarafder S. Calcium phosphate ceramic systems in growth factor and drug delivery for bone tissue engineering: a review. Acta Biomater 2012;8:1401–21.
[37] Sadat-Shojai M, Khorasani MT, Dinpanah-Khoshdargi E, Jamshidi A. Synthesis methods for nanosized hydroxyapatite with diverse structures. Acta Biomater 2013;9:7591–621.
[38] Gomez-Morales J, Iafisco M, Delgado-Lopez JM, Sarda S, Drouet C. Progress on the preparation of nanocrystalline apatites and surface characterization: overview of fundamental and applied aspects. Prog Cryst Growth Charact Mater 2013;59:1–46.
[39] Hayek E, Mullner F, Koller K. Zur kenntnis des hydroxylapatits. Monatsh Chem 1951;82:958–69.
[40] Hayek E, Newesely H, Rumpel ML. Pentacalcium monohydroxyor thophosphate. Inorg Syn 1963;7:63–5.
[41] Termine JD, Posner AS. Calcium phosphate formation in vitro I. Factors affecting initial phase separation. Arch Biochem Biophys 1970;140:307–17.
[42] Eanes ED, Posner AS. A note on the crystal growth of hydroxyapatite precipitated from aqueous solutions. Mater Res Bull 1970;5:377–84.
[43] Jarcho M, Bolen CH, Thomas MB, Bobick J, Kay JF, Doremus RH. Hydroxylapatite synthesis and characterization in dense polycrystalline form. J Mater Sci 1976;11:2027–35.
[44] LeGeros RZ, Trautz OR, LeGeros JP, Klein E, Shirra WP. Apatite crystallites: effects of carbonate on morphology. Science 1967;155:1409–11.
[45] Ivanova TI, Frank-Kamenetskaya OV, Kol'tsov AB, Ugolkov VL. Crystal structure of Ca-deficient carbonated hydroxyapatite. Thermal decomposition. J Solid State Chem 2001;160:340–9.
[46] Habelitz S, Pascual L, Duran A. Nitrogen-containing apatite. J Eur Ceram Soc 1999;19:2685–94.
[47] Bayraktar D, Tas AC. Chemical preparation of carbonated calcium hydroxyapatite powders at 37 °C in urea-containing synthetic body fluid solutions. J Eur Ceram Soc 1999;19:2573–9.
[48] Tas AC. Synthesis of biomimetic Ca-hydroxyapatite powders at 37 °C in synthetic body fluids. Biomaterials 2000;21:1429–38.
[49] Bayraktar D, Tas AC. Formation of hydroxyapatite precursors at 37 °C in urea- and enzyme urease-containing body fluids. J Mater Sci Lett 2001;20:401–3.
[50] Landi E, Tampieri A, Celotti G, Langenati R, Sandri M, Sprio S. Nucleation of biomimetic apatite in synthetic body fluids: dense and porous scaffold development. Biomaterials 2005;26:2835–45.
[51] Bigi A, Ripamonti A, Bruckner S, Gazzano M, Roveri N, Thomas SA. Structure refinements of lead-substituted calcium hydroxyapatite by X-ray powder fitting. Acta Crystallogr B 1989;45:247–51.
[52] Bigi A, Gandolfi M, Gazzano M, Ripamonti A, Roveri N, Thomas SA. Structural modifications of hydroxyapatite induced by lead substitution for calcium. J Chem Soc Dalton 1991;11:2883–6.
[53] Verbeeck RMH, Lassuyt CJ, Heijligers HJM, Driessens FCM, Vrolijk JWGA. Lattice parameters and cation distribution of solid solutions of calcium and lead hydroxyapatite. Calcif Tissue Int 1981;33:243–7.
[54] Ringer S. Concerning the influence exerted by each of the constituents of the blood on the contraction of the ventricle. J Physiol 1882;3:380–93.
[55] Ringer S. A further contribution regarding the influence of the different constituents of the blood on the contraction of the heart. J Physiol 1883;4:29–42.
[56] Ringer S. A third contribution regarding the influence of the inorganic constituents of the blood on the ventricular contraction. J Physiol 1883;4: 222–5.
[57] Rivadeneyra MA, Delgado G, Ramos-Cormenzana A, Delgado R. Biomineralization of carbonates by Halomonas eurihalina in solid and liquid media with different salinities: crystal formation sequence. Res Microbiol 1998;149:277–87.
[58] Rivadeneyra MA, Parraga J, Delgado R, Ramos-Cormenzana A, Delgado G. Biomineralization of carbonates by Halobacillus trueperi in solid and liquid media with different salinities. FEMS Microbiol Ecol 2004;48:39–46.
[59] Delgado G, Parraga J, Martin-Garcia JM, Rivadeneyra MA, Snachez-Maranon M, Delgado R. Carbonate and phosphate precipitation by saline soil bacteria in a monitored culture medium. Geomicrobiol J 2013;30:199–208.
[60] Schmittner KE, Giresse P. Micro-environmental controls on biomineralization: superficial processes of apatite and calcite precipitation in Quaternary soils, Roussillon, France. Sedimentology 1999;46:463–76.
[61] Dupraz S, Parmentier M, Menez B, Guyot F. Experimental and numerical modeling of bacterially induced pH increase and calcite precipitation in saline aquifers. Chem Geol 2009;265:44–53.
[62] Smith MP, Yardley BWD. Fluid evolution during metamorphism of the Otago Schist, New Zealand. (II) Influence of detrital apatite on fluid salinity. J Metamorph Geol 1999;17:187–93.
[63] Pasinli A, Yuksel M, Celik E, Sener S, Tas AC. A new approach in biomimetic synthesis of calcium phosphate coatings using lactic acid–Na lactate buffered body fluid solution. Acta Biomater 2010;6:2282–8.
[64] Miller MA, Kendall MR, Jain MK, Larson PR, Madden AS, Tas AC. Testing of brushite ($CaHPO_4{\cdot}2H_2O$) in synthetic biomineralization solutions and in situ crystallization of brushite micro-granules. J Am Ceram Soc 2012;95:2178–88.
[65] Debye P, Hückel E. The theory of electrolytes I. The lowering of the freezing point and related phenomena. Phys Z 1923;24:185–206.
[66] Marques PAAP, Magalhaes MCF, Correia RN. Inorganic plasma with physiological CO_2/HCO_3^- buffer. Biomaterials 2003;24:1541–8.
[67] Tas AC. Electroless deposition of brushite ($CaHPO_4{\cdot}2H_2O$) crystals on Ti–6Al–4V at room temperature. Int J Mater Res 2006;97:639–44.
[68] Tas AC, Bhaduri SB. Rapid coating of Ti6Al4V at room temperature with a calcium phosphate solution similar to 10× simulated body fluid. J Mater Res 2004;19:2742–9.
[69] Habibovic P, Barrere F, van Blitterswijk CA, de Groot K, Layrolle P. Biomimetic hydroxyapatite coating on metal implants. J Am Ceram Soc 2002;85:517–22.
[70] Watson ML, Robinson RA. Collagen–crystal relationships in bone. II. Electron microscope study of basic calcium phosphate crystals. Am J Anat 1953;93:25–59.
[71] Robinson RA, Watson ML. Crystal–collagen relationships in bone as observed in the electron microscope. III. Crystal and collagen morphology as a function of age. Ann NY Acad Sci 1955;60:596–628.
[72] LeGeros RZ, Trautz OR, Klein E, LeGeros JP. Two types of carbonate substitution in apatite structure. Experientia 1969;25:5–7.
[73] Rey C, Miquel JL, Facchini L, Legrand AP, Glimcher MJ. Hydroxyl groups in bone mineral. Bone 1995;16:583–6.
[74] Loong CK, Rey C, Kuhn LT, Combes C, Wu Y, Chen SH, et al. Evidence of hydroxyl-ion deficiency in bone apatites: an inelastic neutron-scattering study. Bone 2000;26:599–602.

[75] Taylor MG, Parker SF, Simkiss F, Mitchell PCH. Bone mineral: evidence for hydroxy groups by inelastic neutron scattering. Phys Chem Chem Phys 2001;3:1514–7.
[76] Pasteris JD, Wopenka B, Freeman JJ, Rogers K, Valsami-Jones E, van der Houwen JAM, et al. Lack of OH in nanocrystalline apatite as a function of degree of atomic order: implications for bone and biomaterials. Biomaterials 2004;25:229–38.
[77] Alfrey AC, Miller NL, Trow R. Effect of age and magnesium depletion on bone magnesium pools in rats. J Clin Invest 1974;54:1074–81.
[78] Nancollas GH, Tomazic B. Growth of calcium phosphate on hydroxyapatite crystals. Effect of supersaturation and ionic medium. J Phys Chem 1974;78:2218–25.
[79] Bell LC, Posner AM, Quirk JP. The point of zero charge of hydroxyapatite and fluorapatite in aqueous solutions. J Colloid Interface Sci 1973;42:250–61.
[80] Drouet C, Carayon MT, Combes C, Rey C. Surface enrichment of biomimetic apatites with biologically-active ions Mg^{2+} and Sr^{2+}: a preamble to the activation of bone repair materials. Mater Sci Eng C 2008;28:1544–50.
[81] Tas AC, Korkusuz F, Timucin M, Akkas N. An investigation of the chemical synthesis and high-temperature sintering behaviour of calcium hydroxyapatite (HA) and tricalcium phosphate (TCP) bioceramics. J Mater Sci Mater Med 1997;8:91–6.
[82] Posner AS, Betts F. Synthetic amorphous calcium phosphate and its relation to bone mineral structure. Acc Chem Res 1975;8:273–81.
[83] Onuma K, Ito A. Cluster growth model for hydroxyapatite. Chem Mater 1998;10:3346–51.
[84] Combes C, Rey C. Amorphous calcium phosphates: synthesis, properties and uses in biomaterials. Acta Biomater 2010;6:3362–78.
[85] Somrani S, Rey C, Jemal M. Thermal evolution of amorphous tricalcium phosphate. J Mater Chem 2003;13:888–92.
[86] Termine JD, Peckauskas RA, Posner AS. Calcium phosphate formation in vitro. II. Effects of environment on amorphous–crystalline transformation. Arch Biochem Biophys 1970;140:318–25.
[87] Boskey AL, Posner AS. Magnesium stabilization of amorphous calcium phosphate: a kinetic study. Mater Res Bull 1974;9:907–16.
[88] Fowler BO. Infrared studies of apatites. I. Vibrational assignments for calcium, strontium, and barium hydroxyapatites utilizing isotopic substitutions. Inorg Chem 1974;13:194–207.
[89] Fowler BO. Infrared studies of apatites. II. Preparation of normal and isotopically substituted calcium, strontium, and barium hydroxyapatites and spectra–structure–composition correlations. Inorg Chem 1974;13:207–14.
[90] Meyer JL, Fowler BO. Lattice defects in nonstoichiometric hydroxylapatites. A chemical approach. Inorg Chem 1982;21:3029–35.
[91] Knoll M, Ruska E. Das elektronenmikroskop. Z Physik 1932;78:318–39.
[92] Ruska E. The development of the electron microscope and of electron microscopy (Nobel lecture). Angew Chem Int Ed Engl 1987;26:595–605.
[93] Huber L, Rouiller C. Les fibrilles collagenes de l'os (Etude au microscope electronique). Experientia 1951;7:338–40.
[94] Robinson RA, Watson ML. Collagen–crystal relationships in bone as seen in the electron microscope. Anat Rec 1952;114:383–409.
[95] Rouiller C, Huber L, Rutishauser E. La structure de la dentine – étude comparee de l'os et de livoire au microscope electronique. Acta Anat 1952;16:16–28.
[96] Martin RI, Brown PW. The effects of magnesium on hydroxyapatite formation in vitro from $CaHPO_4$ and $Ca_4(PO_4)_2O$ at 37.4 °C. Calcif Tissue Int 1997;60:538–46.
[97] Eanes ED, Hailer AW. Anionic effects on the size and shape of apatite crystals grown from physiological solutions. Calcif Tissue Int 2000;66:449–55.
[98] Tien WB, Chen MT, Yao PC. Effects of pH and temperature on microstructure and morphology of hydroxyapatite/collagen composites synthesized in vitro. Mater Sci Eng C 2012;32:2096–102.
[99] Barbani N, Rosellini E, Cristallini C, Guerra GD, Krajewski A, Mazzocchi M. Hydroxyapatite–collagen composites. Part I. Can the decrease of the interactions between the two components be a physicochemical component of osteoporosis in aged bone? J Mater Sci Mater Med 2011;22:637–46.
[100] Zhang L, Tang P, Xu M, Zhang W, Chai W, Wang Y. Effects of crystalline phase on the biological properties of collagen–hydroxyapatite composites. Acta Biomater 2010;6:2189–99.
[101] Ficai A, Andronescu E, Voicu G, Ghitulica C, Vasile BS, Ficai D, et al. Self-assembled collagen/hydroxyapatite composite materials. Chem Eng J 2010;160:794–800.
[102] Yoshida T, Kikuchi M, Koyama Y, Takakuda K. Osteogenic activity of MG63 cells on bone-like hydroxyapatite/collagen nanocomposite sponges. J Mater Sci Mater Med 2010;21:1263–72.
[103] Sena LA, Caraballo MM, Rossi AM, Soares GA. Synthesis and characterization of biocomposites with different hydroxyapatite–collagen ratios. J Mater Sci Mater Med 2009;20:2395–400.
[104] Liao S, Ngiam M, Chan CK, Ramakrishna S. Fabrication of nano-hydroxyapatite/collagen/osteonectin composites for bone graft applications. Biomed Mater 2009;4:025019.
[105] Teng SH, Lee EJ, Wang P, Kim HE. Collagen/hydroxyapatite composite nanofibers by electrospinning. Mater Lett 2008;62:3055–8.
[106] Yunoki S, Marukawa E, Ikoma T, Sotome S, Fan H, Zhang X, et al. Effect of collagen fibril formation on bioresorbability of hydroxyapatite/collagen composites. J Mater Sci Mater Med 2007;18:2179–83.
[107] Watanabe K, Nishio Y, Makiura R, Nakahira A, Kojima C. Paclitaxel-loaded hydroxyapatite/collagen hybrid gels as drug delivery systems for metastatic cancer cells. Int J Pharm 2013;446:81–6.
[108] Jia L, Duan Z, Fan D, Mi Y, Hui J, Chang L. Human-like collagen/nano-hydroxyapatite scaffolds for the culture of chondrocytes. Mater Sci Eng C 2013;33:727–34.
[109] Sionkowska A, Kozlowska J. Properties and modification of 3-D collagen/hydroxyapatite composites. Int J Biol Macromol 2013;52:250–9.
[110] Song W, Markel DC, Jin X, Shi T, Ren W. Poly(vinyl alcohol)/collagen/hydroxyapatite hydrogel: properties and in vitro cellular response. J Biomed Mater Res 2012;100A:3071–9.
[111] Song W, Markel DC, Wang S, Shi T, Mao G, Ren W. Electrospun polyvinyl alcohol–collagen–hydroxyapatite nanofibers: a biomimetic extracellular matrix for osteoblastic cells. Nanotechnology 2012;23:115101.
[112] Curtin CM, Cunniffe GM, Lyons FG, Bessho K, Dickson GR, Duffy GP, et al. Innovative collagen nano-hydroxyapatite scaffolds offer a highly efficient non-viral gene delivery platform for stem cell-mediated bone formation. Adv Mater 2012;24:749–54.
[113] Phipps MC, Clem WC, Grunda JM, Clines GA, Bellis SL. Increasing the pore sizes of bone-mimetic electrospun scaffolds comprised of polycaprolactone, collagen I and hydroxyapatite to enhance cell infiltration. Biomaterials 2012;33:524–34.
[114] Heinemann S, Heinemann C, Jaeger M, Neunzehn J, Wiesmann HP, Hanke T. Effect of silica and hydroxyapatite mineralization on the mechanical properties and the biocompatibility of nanocomposite collagen scaffolds. Appl Mater Interfaces 2011;3:4323–31.
[115] Zhou J, Xu C, Wu G, Cao X, Zhang L, Zhai Z, et al. In vitro generation of osteochnodral differentiation of human marrow mesenchymal stem cells in novel collagen–hydroxyapatite layered scaffolds. Acta Biomater 2011;7:3999–4006.
[116] Teixeira S, Fernandes MH, Ferraz MP, Monteiro FJ. Proliferation and mineralization of bone marrow cells cultured on macroporous hydroxyxapatite scaffolds functionalized with collagen type I for bone tissue regeneration. J Biomed Mater Res 2010;95A:1–8.
[117] Cunniffe GM, Dickson GR, Partap S, Stanton KT, O'Brien FJ. Development and characterisation of a collagen nano-hydroxyapatite composite scaffold for bone tissue engineering. J Mater Sci Mater Med 2010;21:2293–8.
[118] Teixeira S, Yang L, Dijkstra PJ, Ferraz MP, Monteiro FJ. Heparinized hydroxyapatite/collagen three-dimensional scaffolds for tissue engineering. J Mater Sci Mater Med 2010;21:2385–92.
[119] Liu Y, Williams DJ. Incorporation of hydroxyapatite sol into collagen gel to regulate the contraction mediated by human bone marrow-derived stromal cells. IEEE Trans Nanobiosci 2010;9:1–11.
[120] Wang Y, Zhang L, Hu M, Liu H, Wen W, Xiao H, et al. Synthesis and characterization of collagen–chitosan–hydroxyapatite artificial bone matrix. J Biomed Mater Res 2008;86A:244–52.
[121] Wahl DA, Sachlos E, Liu C, Czernuszka JT. Controlling the processing of collagen–hydroxyapatite scaffolds for bone tissue engineering. J Mater Sci Mater Med 2007;18:201–9.
[122] Rammelt S, Neumann M, Hanisch U, Reinstorf A, Pompe W, Zwipp H, et al. Osteocalcin enhances bone remodeling around hydroxyapatite/collagen composites. J Biomed Mater Res 2005;73A:284–94.
[123] Ficai A, Albu MG, Birsan M, Sonmez M, Ficai D, Trandafir V, et al. Collagen hydrolysate based collagen/hydroxyapatite composite materials. J Mol Struct 2013;1037:154–9.
[124] Wei Q, Lu J, Ai H, Jiang B. Novel method for the fabrication of multiscale structure collagen/hydroxyapatite-microsphere composites based on $CaCO_3$ microparticle templates. Mater Lett 2012;80:91–4.
[125] Shen X, Chen L, Cai X, Tong T, Tong H, Hu J. A novel method for the fabrication of homogeneous hydroxyapatite/collagen nanocomposite and nanocomposite scaffold with hierarchical porosity. J Mater Sci Mater Med 2011;22:299–305.
[126] Zhao H, Huang C, Jin H, Cai J. A novel route for collagen/hydroxyapatite preparation by enzymatic decomposition of urea. J Compos Mater 2010;44:2127–33.
[127] Ehrlich H, Hanke T, Simon P, Born R, Fischer C, Frolov A, et al. Carboxymethylation of the fibrillar collagen with respect to formation of hydroxyapatite. J Biomed Mater Res 2010;92B:542–51.
[128] Pelin IM, Maier SS, Chitanu GC, Bulacovschi V. Preparation and characterization of a hydroxyapatite–collagen composite as component for injectable bone substitute. Mater Sci Eng C 2009;29:2188–94.
[129] Kuroda K, Moriyama M, Ichino R, Okido M, Seki A. Formation and osteoconductivity of hydroxyapatite/collagen composite films using a thermal substrate method in aqueous solutions. Mater Trans 2009;50:1190–5.
[130] Zhai Y, Cui FZ. Recombinant human-like collagen directed growth of hydroxyapatite nanocrystals. J Cryst Growth 2006;291:202–6.
[131] Goissis G, Maginador SVS, Martins VCA. Biomimetic mineralization of charged collagen matrices: in vitro and in vivo study. Artif Organs 2003;27:437–43.
[132] Rosseeva EV, Buder J, Simon P, Schwarz U, Frank-Kamenetskaya OV, Kniep R. Synthesis, characterization, and morphogenesis of carbonated fluorapatite-gelatine nanocomposites: a complex biomimetic approach toward the mineralization of hard tissues. Chem Mater 2008;20:6003–13.
[133] Li H, Guo Z, Xue B, Zhang Y, Huang W. Collagen modulating crystallization of apatite in a biomimetic gel system. Ceram Int 2011;37:2305–10.

[134] Zahn D, Hochrein O, Kawska A, Brickmann J, Kniep R. Towards an atomistic understanding of apatite–collagen biomaterials: linking molecular simulation studies of complex-, crystal- and composite-formation to experimental findings. J Mater Sci 2007;42:8966–73.

[135] Almora-Barrios N, De Leeuw NH. Molecular dynamics simulation of the early stages of the nucleation of hydroxyapatite at a collagen template. Cryst Growth Des 2012;12:756–63.

[136] Antebi B, Cheng X, Harris JN, Gower LB, Chen XD, Ling J. Biomimetic collagen–hydroxyapatite composite fabricated via a novel perfusion-flow mineralization technique. Tissue Eng Part C 2013;19:487–96.

[137] Gower LB. Biomimetic model systems for investigating the amorphous precursor pathway and its role in biomineralization. Chem Rev 2008;108:4551–627.

[138] Bradt JH, Mertig M, Teresiak A, Pompe W. Biomimetic mineralization of collagen by combined fibril assembly and calcium phosphate formation. Chem Mater 1999;11:2694–701.

[139] Deshpande AS, Beniash E. Bioinspired synthesis of mineralized collagen fibrils. Cryst Growth Des 2008;8:3084–90.

[140] Nudelman F, Pieterse K, George A, Bomans PHH, Friedrich H, Brylka LJ, et al. The role of collagen in bone apatite formation in the presence of hydroxyapatite nucleation inhibitors. Nat Mater 2010;9:1004–9.

[141] Lickorish D, Ramshaw JAM, Werkmeister JA, Glattauer V, Howlett CR. Collagen–hydroxyapatite composite prepared by biomimetic process. J Biomed Mater Res 2004;68A:19–27.

[142] Jalota S, Bhaduri SB, Tas AC. Using a synthetic body fluid (SBF) solution of 27 mM HCO_3^- to make bone substitutes more osteointegrative. Mater Sci Eng C 2008;28:129–40.

[143] Al-Munajjed AA, Plunkett NA, Gleeson JP, Weber T, Jungreuthmayer C, Levingstone T, et al. Development of a biomimetic collagen–hydroxyapatite scaffold for bone tissue engineering using a SBF immersion technique. J Biomed Mater Res 2009;90B:584–91.

[144] Ficai A, Andronescu E, Voicu G, Albu MG, Ilie A. Biomimetic synthesis of collagen/hydroxyapatite composite materials. Mater Plast 2010;47:205–8.

[145] Wang Y, Azais T, Robin M, Vallee A, Catania C, Legriel P, et al. The predominant role of collagen in the nucleation, growth, structure and orientation of bone apatite. Nat Mater 2012;11:724–33.

[146] Barrere F, Layrolle P, van Blitterswijk CA, de Groot K. Biomimetic calcium phosphate coatings on Ti6Al4V: a crystal growth study of octacalcium phosphate and inhibition by Mg^{2+} and HCO_3^-. Bone 1999;25:107S–11S.

[147] Hohling HJ, Kreilos R, Neubauer G, Boyde A. Electron microscopy and electron microscopical measurements of collagen mineralization in hard tissues. Z Zellforsch Mik Anat 1971;122:36–52.

[148] Hohling HJ, Ashton BA, Koster HD. Quantitative electron microscopic investigations of mineral nucleation in collagen. Cell Tissue Res 1974;148:11–26.

[149] Abbona F, Baronnet A. A XRD and TEM study on the transformation of amorphous calcium phosphate in the presence of magnesium. J Cryst Growth 1996;165:98–105.

[150] Brecevic L, Hlady V, Furedi-Milhofer H. Influence of gelatin on the precipitation of amorphous calcium phosphate. Colloid Surface 1987;28:301–13.

[151] Christoffersen J, Christoffersen MR, Kibalczyc W, Andersen FA. A contribution to the understanding of the formation of calcium phosphates. J Cryst Growth 1989;94:767–77.

[152] Fleisch H. Inhibitors of calcium phosphate precipitation and their role in biological mineralization. J Cryst Growth 1981;53:120–34.

[153] Kim S, Ryu HS, Shin H, Jung HS, Hong KS. In situ observation of hydroxyapatite nanocrystal formation from amorphous calcium phosphate in calcium-rich solutions. Mater Chem Phys 2005;91:500–6.

[154] Ofir PBY, Govrin-Lippman R, Garti N, Furedi-Milhofer H. The influence of polyelectrolytes on the formation and phase transformation of amorphous calcium phosphate. Cryst Growth Des 2004;4:177–83.

[155] Tao JH, Pan HH, Zeng YW, Xu XR, Tang RK. Roles of amorphous calcium phosphate and biological additives in the assembly of hydroxyapatite nanoparticles. J Phys Chem B 2007;111:13410–8.

[156] Pan HH, Liu XY, Tang RK, Xu HY. Mystery of the transformation from amorphous calcium phosphate to hydroxyapatite. Chem Commun 2010;46:7415–7.

[157] Zyman Z, Rokhmistrov D, Glushko V. Structural changes in precipitates and cell model for the conversion of amorphous calcium phosphate to hydroxyapatite during the initial stage of precipitation. J Cryst Growth 2012;353:5–11.

[158] Kazanci M, Fratzl P, Klaushofer K, Paschalis EP. Complementary information on in vitro conversion of amorphous (precursor) calcium phosphate to hydroxyapatite from Raman microspectroscopy and wide-angle X-ray scattering. Calcif Tissue Int 2006;79:354–9.

[159] Blumenthal NC, Holmes JM, Posner AS. Effect of preparation conditions on the properties and transformation of amorphous calcium phosphate. Mater Res Bull 1972;7:1181–90.

[160] Meyer JL, Weatherall CC. Amorphous to crystalline calcium phosphate transformation at elevated pH. J Colloid Interface Sci 1982;89:257–67.

[161] Tung MS, Brown WE. An intermediate state in hydrolysis of amorphous calcium phosphate. Calcif Tissue Int 1983;35:783–90.

[162] Tas AC. Calcium metal to synthesize amorphous or cryptocrystalline calcium phosphates. Mater Sci Eng C 2012;32:1097–106.

[163] Reid DG, Duer MJ, Murray RC, Wise ER. The organic–mineral interface in teeth is like that in bone and dominated by polysaccharides: universal mediators of normal calcium phosphate biomineralization in vertebrates? Chem Mater 2008;20:3549–50.

[164] Baskett TF. Sydney Ringer and lactated Ringer's solution. Resuscitation 2003;58:5–7.

[165] Miller DJ. Sydney Ringer; physiological saline, calcium and the contraction of the heart. J Physiol 2004;555:585–7.

[166] Lockwood APM. "Ringer" solutions and some notes on the physiological basis of their ionic composition. Comp Biochem Physiol 1961;2:241–89.

[167] Locke FS. Towards the ideal artificial circulating fluid for the isolated frog's heart. J Physiol 1895;18:332–3.

[168] Locke FS. Die Wirkung der Metalle das Blutplasmas und verschiedener Zucker auf des isoliertes Sauegetierherz. Zbl Physiol 1900;14:670.

[169] Lee JA. Sydney Ringer (1834–1910) and Alexis Hartmann (1898–1964). Anaesthesia 1981;36:1115–21.

[170] Hartmann AF, Senn MJE. Studies in the metabolism of sodium r-lactate. II. Response of human subjects with acidosis to the intravenous injection of sodium *r*-lactate. J Clin Invest 1932;11:337–44.

[171] Darrow DC, Yannet H. The changes in the distribution of body water accompanying increase and decrease in extracellular electrolytes. J Clin Invest 1935;14:266–75.

[172] Canizaro PC, Prager MD, Shires GT. The infusion of Ringer's lactate solution during shock – changes in lactate, excess lactate, and pH. Am J Surgery 1971;122:494–501.

[173] Moore FA. The use of lactated Ringer's in shock resuscitation: the good, the bad and the ugly. J Trauma 2011;70:S15–6.

[174] Hu X, Zhai X, Hirt T. A new concept for more biocompliant bone cements for vertebroplasty and kyphoplasty. Macromol Biosci 2009;9:195–202.

[175] Huan Z, Chang J. Effect of sodium carbonate solution on self-setting properties of tricalcium bone cement. J Biomater Appl 2008;23:247–62.

[176] Khairoun I, Billon A, Daculsi G, Merle C, Bouler JM. Improvement of porosity of a calcium phosphate cement by incorporation of biodegradable polymer microspheres. Key Eng Mater 2005;284–286:129–32.

[177] Fernandez E, Gil FJ, Best S, Ginebra MP, Driessens FCM, Planell JA. The cement setting reaction in the $CaHPO_4$–α-$Ca_3(PO_4)_2$ system: an X-ray diffraction study. J Biomed Mater Res 1998;42:403–6.

[178] Fernandez E, Ginebra MP, Boltong MG, Driessens FCM, Ginebra J, De Maeyer EAP, et al. Kinetic study of the setting reaction of a calcium phosphate bone cement. J Biomed Mater Res 1996;32:367–74.

[179] Ginebra MP, Fernandez E, Driessens FCM, Boltong MG, Muntasell J, Font J, et al. The effects of temperature on the behavior of an apatitic calcium phosphate bone cement. J Mater Sci Mater Med 1995;6:857–60.

[180] Driessens FCM, Boltong MG, Bermudez O, Planell HA, Ginebra MP, Fernandez E. Effective formulations for the preparation of calcium phosphate bone cements. J Mater Sci Mater Med 1994;5:164–70.

[181] Hsu YH, Turner IG, Miles AW. Mechanical properties of three different compositions of calcium phosphate bioceramic following immersion in Ringer's solution and distilled water. J Mater Sci Mater Med 2009;20:2367–74.

[182] Jun YK, Kim WH, Kweon OK, Hong SH. The fabrication and biochemical evaluation of alumina reinforced calcium phosphate porous implants. Biomaterials 2003;24:3731–9.

[183] Kwon SH, Jun YK, Hong SH, Kim HE. Synthesis and dissolution behavior of β-TCP and HA/β-TCP composite powders. J Eur Ceram Soc 2003;23:1039–45.

[184] Raynaud S, Champion E, Lafon JP, Bernache-Assollant D. Calcium phosphate apatites with variable Ca/P atomic ratio III. Mechanical properties and degradation in solution of hot pressed ceramics. Biomaterials 2002;23:1081–9.

[185] Mansur C, Pope M, Pascucci MR, Shivkumar S. Zirconia–calcium phosphate composites for bone replacement. Ceram Int 1998;24:77–9.

[186] Hsu CK, Lee JS, Sheu JM, Huang CW. Physical properties of calcium phosphate glasses with various CaO/P_2O_5 mole ratios. Phosphorus Sulfur 1996;109–110:47–50.

[187] Gopi D, Ramya S, Rajeswari D, Kavitha L. Corrosion protection performance of porous strontium hydroxyapatite coating on polypyrrole coated 316L stainless steel. Colloid Surface B 2013;107:130–6.

[188] Drevet R, Nzoghe-Mendome L, Benhayoune H, Ebothe J. Nanoscale surface modification of a prosthetic material: case of Ti6Al4V into Ringer's solution. J Nanosci Nanotechnol 2012;12:4956–61.

[189] Simka W, Sadkowski A, Warczak M, Iwaniak A, Dercz G, Michalska J, et al. Characterization of passive films formed on titanium during anodic oxidation. Electrochim Acta 2011;56:8962–8.

[190] Sun F, Sask KN, Brash JL, Zhitomirsky I. Surface modifications of Nitinol for biomedical applications. Colloid Surface B 2008;67:132–9.

[191] Natarajan UV, Rajeswari S. Influence of calcium precursors on the morphology and crystallinity of sol–gel-derived hydroxyapatite nanoparticles. J Cryst Growth 2008;310:4601–11.

[192] Alkhateeb A, Virtanen S. Influence of surface self-modification in Ringer's solution on the passive behavior of titanium. J Biomed Mater Res 2005;75A:934–40.

[193] Gledhill HC, Turner IG, Doyle C. In vitro dissolution behavior of two morphologically different thermally sprayed hydroxyapatite coatings. Biomaterials 2001;22:695–700.

[194] Mukherjee DP, Dorairaj NR, Mills DK, Graham D, Krauser JT. Fatigue properties of hydroxyapatite-coated dental implants after exposure to a periodontal pathogen. J Biomed Mater Res 2000;53:467–74.

[195] Campbell PA, Gledhill HC, Brown SR, Turner IG. Vacuum plasma sprayed hydroxyapatite coatings on titanium alloy substrates: surface characterization and observation of dissolution processes using atomic force microscopy. J Vac Sci Technol B 1996;14:1167–72.

[196] Burstein GT, Liu C, Souto RM. The effect of temperature on the nucleation of corrosion pits on titanium in Ringer's physiological solution. Biomaterials 2005;26:245–56.

[197] MacConaill M. Calcium precipitation from mammalian physiological salines (Ringer solutions) and the preparation of high [Ca] media. J Pharmacol Method 1985;14:147–55.

[198] Tyrode MV. The mode of action of some purgative salts. Arch Int Pharmacod T 1910;20:205–23.

[199] Krebs HA, Henseleit K. Untersuchungen ueber die Harnstoffbildung im Tierkoerper. Hoppe-Seylers Z Physiol Chem 1932;210:33–66.

[200] Earle WR. Production of malignancy in vitro. IV. The mouse fibroblast cultures and changes seen in the living cells. J Nat Cancer Inst 1943;4:165–212.

[201] Evans VJ, Bryant JC, Fioramonti MC, McQuilkin WT, Sanford KK, Earle WR. Studies of nutrient media for tissue cells in vitro. I. A protein-free chemically defined medium for cultivation of strain L cells. Cancer Res 1956;16:77–86.

[202] Evans VJ, Bryant JC, Fioramonti MC, McQuilkin WT, Sanford KK, Westfall BB, et al. Studies of nutrient media for tissue cells in vitro. II. An improved protein-free chemically defined medium for long-term cultivation of strain L-929 cells. Cancer Res 1956;16:87–95.

[203] Termine JD, Eanes ED. Calcium phosphate deposition from balanced salt solutions. Calcif Tiss Res 1974;15:81–4.

[204] Eanes ED. The interaction of supersaturated calcium phosphate solutions with apatitic substrates. Calcif Tiss Res 1976;20:75–89.

[205] Tuck L, Astala R, Reid JW, Sayer M, Stott MJ. Dissolution and re-crystallization processes in multiphase silicon stabilized tricalcium phosphate. J Mater Sci Mater Med 2008;19:917–27.

[206] Tas AC. A new calcium phosphate cement composition and a method for the preparation thereof. US Patent 6,929,692, European Patent 1,394,132, Canadian Patent 2,438,742.

[207] Shadanbaz S, Walker J, Staiger MP, Dias GJ, Pietak A. Growth of calcium phosphates on magnesium substrates for corrosion control in biomedical applications via immersion techniques. J Biomed Mater Res 2013;101B:162–72.

[208] Hanks JH, Wallace RE. Relation of oxygen and temperature in the preservation of tissues by refrigeration. Proc Soc Exp Biol Med 1949;71:196–200.

[209] Hanks JH. The longevity of chick tissue cultures without renewal of medium. J Cell Comp Physiol 1948;31:235–60.

[210] Huigen YM, Krips HJ, Hulleman S, Gelsema WJ, de Ligny CL. The adsorption of ^{99m}Tc(Sn)–diphosphonate complexes on tri-calcium phosphate: the influence of preparation conditions, ligand-type, incubation media and adsorption conditions. The reversibility of the adsorption. Appl Radiat Isot 1990;41:189–94.

[211] Kummer FJ, Jaffe WL. Stability of a cyclically loaded hydroxyapatite coating: effect of substrate material, surface preparation, and testing environment. J Appl Biomater 1992;3:211–5.

[212] Maxian SH, Zawadsky JP, Dunn MG. In vitro evaluation of amorphous calcium phosphate and poorly crystallized hydroxyapatite coatings on titanium implants. J Biomed Mater Res 1993;27:111–7.

[213] Yoshinari M, Ohtsuka Y, Derand T. Thin hydroxyapatite coating produced by the ion beam dynamic mixing method. Biomaterials 1994;15:529–35.

[214] Leitao E, Barbosa MA, de Groot K. In vitro calcification of orthopaedic implant materials. J Mater Sci Mater Med 1995;6:849–52.

[215] Reis RL, Monteiro FJ. Crystallinity and structural changes in HA plasma-sprayed coatings induced by cyclic loading in physiological media. J Mater Sci Mater Med 1996;7:407–11.

[216] Sousa SR, Barbosa MA. Effect of hydroxyapatite thickness on metal ion release from Ti6Al4V substrates. Biomaterials 1996;17:397–404.

[217] Hanawa T, Kon M, Ukai H, Murakami K, Miyamoto Y, Asaoka K. Surface modification of titanium in calcium-ion-containing solutions. J Biomed Mater Res 1997;34:273–8.

[218] Wen HB, de Wijn JR, Cui FZ, de Groot K. Preparation of calcium phosphate coatings on titanium implant materials by simple chemistry. J Biomed Mater Res 1998;41:227–36.

[219] Frauchiger L, Taborelli M, Aronsson BO, Descouts P. Ion adsorption on titanium surfaces exposed to a physiological solution. Appl Surf Sci 1999;143:67–77.

[220] Haynes JA, Rigney ED, Janowski GM. Effects of cyclic bending and physiological solution on plasma-sprayed hydroxylapatite coatings of varying crystallinity. J Biomed Mater Res 1999;48:403–10.

[221] Kirk PB, Filiaggi MJ, Sodhi RNS, Pilliar RM. Evaluating sol–gel ceramic thin films for metal implant applications. III. In vitro aging of sol–gel-derived zirconia films on Ti–6Al–4V. J Biomed Mater Res 1999;48:424–33.

[222] Serro APVA, Fernandes AC, Saramago BJV. Calcium phosphate deposition on titanium surfaces in the presence of fibronectin. J Biomed Mater Res 2000;49:345–52.

[223] Grassmann O, Heimann RB. Compositional and microstructural changes engineered plasma-sprayed hydroxyapatite coatings on Ti6Al4V substrates during incubation in protein-free simulated body fluid. J Biomed Mater Res 2000;53:685–93.

[224] Lima J, Sousa SR, Ferreira A, Barbosa MA. Interactions between calcium, phosphate, and albumin on the surface of titanium. J Biomed Mater Res 2001;55:45–53.

[225] Al-Abdullat Y, Tsutsumi S, Nakajima N, Ohta M, Kuwahara H, Ikeuchi K. Surface modification of magnesium by $NaHCO_3$ and corrosion behavior in Hank's solution for new biomaterial applications. Mater Trans 2001;42:1777–80.

[226] Heimann RB, Grassmann O, Zumbrink T, Jennissen HP. Biomimetic processes during in vitro leaching of plasma-sprayed hydroxyapatite coatings for endoprosthetic applications. Materialwiss Werkst 2001;32:913–21.

[227] Metikos-Hukovic M, Kwokal A, Piljac J. The influence of niobium and vanadium on passivity of titanium-based implants in physiological solution. Biomaterials 2003;24:3765–75.

[228] Yang YC, Chang E, Lee SY. Mechanical properties and Young's modulus of plasma-sprayed hydroxyapatite coating on Ti substrate in simulated body fluid. J Biomed Mater Res 2003;67A:886–99.

[229] Hiromoto S, Hanawa T, Asami K. Composition of surface oxide film of titanium with culturing murine fibroblasts L929. Biomaterials 2004;25:979–86.

[230] Kuo MC, Yen SK. Immersion characteristics of electrolytic calcium phosphate coated Ti in simulated physiological fluid. J Mater Sci 2004;39:2357–63.

[231] Tanaka Y, Kobayashi E, Hiromoto S, Asami K, Imai H, Hanawa T. Calcium phosphate formation on titanium by low-voltage electrolytic treatments. J Mater Sci Mater Med 2007;18:797–806.

[232] Ohtsu N, Sato K, Saito K, Asami K, Hanawa T. Calcium phosphates formation on $CaTiO_3$ coated titanium. J Mater Sci Mater Med 2007;18:1009–16.

[233] Hiromoto S, Shishido T, Yamamoto A, Maruyama N, Somekawa H, Mukai T. Precipitation control of calcium phosphate on pure magnesium by anodization. Corrosion Sci 2008;50:2906–13.

[234] Geng F, Tan LL, Jin XX, Jang JY, Yang K. The preparation, cytocompatibility, and in vitro biodegradation study of pure β-TCP on magnesium. J Mater Sci Mater Med 2009;20:1149–57.

[235] Yan ZC, Chang ZR, Long LC, Cheng GJ. Comparison of calcium phosphate coatings on Mg–Al and Mg–Ca alloys and their corrosion behavior in Hank's solution. Surf Coat Technol 2010;204:3636–40.

[236] Popa MV, Moreno JMC, Popa M, Vasilescu E, Drob P, Vasilescu C, et al. Electrochemical deposition of bioactive coatings on Ti and Ti–6Al–4V surfaces. Surf Coat Technol 2011;205:4776–83.

[237] Waterman J, Pietak A, Birbilis N, Woodfield T, Dias G, Staiger MP. Corrosion resistance of biomimetic calcium phosphate coatings on magnesium due to varying pretreatment time. Mater Sci Eng B 2011;176:1756–60.

[238] Roland T, Pelletier H, Krier J. Scratch resistance and electrochemical corrosion behavior of hydroxyapatite coatings on Ti6Al4V in simulated physiological media. J Appl Electrochem 2013;43:53–63.

[239] Milosev I, Hmeljak J, Cor A. Hyaluronic acid stimulates the formation of calcium phosphate on CoCrMo alloy in simulated physiological solution. J Mater Sci Mater Med 2013;24:555–71.

[240] Jha LJ, Santos JD, Knowles JC. Characterization of apatite layer formation on P_2O_5–CaO, P_2O_5–CaO–Na_2O, and P_2O_5–CaO–Na_2O–Al_2O_3 glass hydroxyapatite composites. J Biomed Mater Res 1996;31:481–6.

[241] Kumar M, Xie J, Chittur K, Riley C. Transformation of modified brushite to hydroxyapatite in aqueous solution: effects of potassium substitution. Biomaterials 1999;20:1389–99.

[242] Xie J, Riley C, Chittur K. Effect of albumin on brushite transformation to hydroxyapatite. J Biomed Mater Res 2001;57:357–65.

[243] Serro AP, Fernandes AC, Saramago B, Fernandes MHV. In vitro mineralization of a glass-ceramic of the MgO–3CaO·P_2O_5–SiO_2 system: wettability studies. J Biomed Mater Res 2002;61:99–108.

[244] Marques PAAP, Serro AP, Saramago BJ, Fernandes AC, Magalhaes MCF, Correia RN. Mineralisation of two calcium phosphate ceramics in biological model fluids. J Mater Chem 2003;13:1484–90.

[245] Hirakata LM, Kon M, Asaoka K. Evaluation of apatite ceramics containing α-tricalcium phosphate by immersion in simulated body fluid. Biomed Mater Eng 2003;13:247–59.

[246] Marques PAAP, Serro AP, Saramago BJ, Fernandes AC, Magalhaes MCF, Correia RN. Mineralisation of two phosphate ceramics in HBSS: role of albumin. Biomaterials 2003;24:451–60.

[247] Chen WC, Lin JHC, Ju CP. Transmission electron microscopic study on setting mechanism of tetracalcium phosphate/dicalcium phosphate anhydrous-based calcium phosphate cement. J Biomed Mater Res 2003;64A:664–71.

[248] Yadav KL, Brown PW. Formation of hydroxyapatite in water, Hank's solution, and serum at physiological temperature. J Biomed Mater Res 2003;65A:158–63.

[249] Hayakawa T, Yoshinari M, Sakae T, Nemoto K. Calcium phosphate formation on the phosphorylated dental bonding agent in electrolyte solution. J Oral Rehabil 2004;31:67–73.

[250] Krajewski A, Ravaglioli A, Tinti A, Taddei P, Mazzocchi M, Martinetti R, et al. Comparison between the in vitro surface transformations of AP40 and RKKP bioactive glasses. J Mater Sci Mater Med 2005;16:119–28.

[251] Tanimoto Y, Hayakawa T, Sakae T, Nemoto K. Characterization and bioactivity of tape-cast and sintered TCP sheets. J Biomed Mater Res 2006;76A:571–9.

[252] Chen WC, Ju CP, Lin JHC. Variation in structure and properties of a non-dispersive TTCP/DCPA-derived CPC immersed in Hanks' solution. J Oral Rehabil 2007;34:541–51.

[253] Ding SJ. Biodegradation behavior of chitosan/calcium phosphate composites. J Non-Cryst Solids 2007;353:2367–73.

[254] Hesaraki S, Moztarzadeh F, Sharifi D. Formation of interconnected macropores in apatitic calcium phosphate bone cement with the use of an effervescent additive. J Biomed Mater Res 2007;83A:80–7.
[255] Miyai T, Ito A, Tamazawa G, Matsuno T, Sogo Y, Nakamura C, et al. Antibiotic-loaded poly-ε-caprolactone and porous β-tricalcium phosphate composite for treating osteomyelitis. Biomaterials 2008;29:350–8.
[256] Tsai CH, Ju CP, Lin JHC. Morphology and mechanical behavior of TTCP-derived calcium phosphate cement subcutaneously implanted in rats. J Mater Sci Mater Med 2008;19:2407–15.
[257] Sato M, Tu R, Goto T, Ueda K, Narushima T. Precipitation behavior in a Hanks' solution on Ca–P–O films prepared by laser CVD. Mater Trans 2009;50:2455–9.
[258] Taddei P, Tinti A, Gandolfi MG, Rossi PL, Prati C. Ageing of calcium silicate cements for endodontic use in simulated body fluids: a micro-Raman study. J Raman Spectrosc 2009;40:1858–66.
[259] Gandolfi MG, Taddei P, Tinti A, Dorigo ES, Rossi PL, Prati C. Kinetics of apatite formation on a calcium–silicate cement for root-end filling during ageing physiological-like phosphate solutions. Clin Oral Invest 2010;14:659–68.
[260] Roguska A, Pisarek M, Andrzejczuk M, Dolata M, Lewandowska M, Janik-Czachor M. Characterization of a calcium phosphate–TiO_2 nanotube composite layer for biomedical applications. Mater Sci Eng C 2011;31:906–14.
[261] Nath S, Tu R, Goto T. Apatite formation in Hanks' solution on β-Ca_2SiO_4 films prepared by MOCVD. Surf Coat Technol 2011;206:172–7.
[262] Kim TW, Park YM, Kim DH, Jin HH, Shin KK, Jung JS, et al. In situ formation of biphasic calcium phosphates and their biological performance in vivo. Ceram Int 2012;38:1965–74.
[263] Kim TW, Lee HS, Kim DH, Jin HH, Hwang KH, Lee JK, et al. In situ synthesis of magnesium-substituted biphasic calcium phosphate and in vitro biodegradation. Mater Res Bull 2012;47:2506–12.
[264] Eagle H. Amino acid metabolism in mammalian cell cultures. Science 1959;130:432–7.
[265] Eagle H. Nutrition needs of mammalian cells in tissue culture. Science 1955;122:501–4.
[266] Steinman HG, Eagle H, Oyama VI. The nutritional requirements of treponemata III. A defined medium for cultivation of the Reiter treponeme. J Bacteriol 1952;64:265–9.
[267] Bartter FC. Regulation of the volume and composition of extracellular and intracellular fluid. Ann NY Acad Sci 1963;110:682–703.
[268] Dulbecco R, Freeman G. Plaque production by the polyoma virus. Virology 1959;8:396–7.
[269] Sachs L, Fogel M, Winocour E. In vitro analysis of a mammalian tumour virus. Nature 1959;183:663–4.
[270] Tas AC. X-ray-amorphous calcium phosphate (ACP) synthesis in a simple biomineralization medium. J Mater Chem B 2013;1:4511–20.
[271] Combes C, Rey C, Freche M. In vitro crystallization of octacalcium phosphate on type I collagen: influence of serum albumin. J Mater Sci Mater Med 1999;10:153–60.
[272] Greenfield DJ, Termine JD, Eanes ED. A chemical study of apatites prepared by hydrolysis of amorphous calcium phosphates in carbonate-containing aqueous solutions. Calcif Tiss Res 1974;14:131–8.
[273] Cisar JO, Xu DQ, Thompson J, Swaim W, Hu L, Kopecko DJ. An alternative interpretation of nanobacteria-induced biomineralization. PNAS 2000;97:11511–5.
[274] Rao RR, Jiao A, Kohn DH, Stegemann JP. Exogenous mineralization of cell-seeded and unseeded collagen–chitosan hydrogels using modified culture medium. Acta Biomater 2012;8:1560–5.
[275] Gomes S, Renaudin G, Jallot E, Nedelec JM. Structural characterization and biological fluid interaction of sol–gel derived Mg-substituted biphasic calcium phosphate ceramics. Appl Mater Interfaces 2009;1:505–13.
[276] Mandel S, Tas AC. Brushite ($CaHPO_4{\cdot}2H_2O$) to octacalcium phosphate ($Ca_8(HPO_4)_2(PO_4)_4{\cdot}5H_2O$) transformation in DMEM solutions at 36.5 °C. Mater Sci Eng C 2010;30:245–54.
[277] Lee JTY, Leng Y, Chow KL, Ren F, Ge X, Wang K, et al. Cell culture medium as an alternative to conventional simulated body fluid. Acta Biomater 2011;7:2615–22.
[278] Lutisanova G, Palou MT, Kozankova J. Comparison of bioactivity in vitro of glass and glass ceramic materials during soaking in SBF and DMEM medium. Ceram Silikaty 2011;55:199–207.
[279] Lutisanova G, Palou MT, Kozankova J. Mechanism of bioactivity of LS2-FA glass-ceramics in SBF and DMEM medium. Ceram Silikaty 2012;56:229–37.
[280] Declercq HA, Verbeeck RMH, DeRidder LIFJM, Schacht EH, Cornelissen MJ. Calcification as an indicator of osteoinductive capacity of biomaterials in osteoblastic cell cultures. Biomaterials 2005;26:4964–74.
[281] Faure J, Balamurugan A, Benhayoune H, Torres P, Balossier G, Ferreira JMF. Morphological and chemical characterization of biomimetic bone like apatite formation on alkali treated Ti6Al4V titanium alloy. Mater Sci Eng C 2009;29:1252–7.
[282] Dumelie N, Benhayoune H, Richard D, Laurent-Maquin D, Balossier G. In vitro precipitation of electrodeposited calcium-deficient hydroxyapatite coatings on Ti6Al4V substrate. Mater Charact 2008;59:129–33.
[283] Drevet R, Velard F, Potiron S, Laurent-Maquin D, Benhayoune H. In vitro dissolution and corrosion study of calcium phosphate coatings elaborated by pulsed electrodeposition current on Ti6Al4V substrate. J Mater Sci Mater Med 2011;22:753–61.
[284] Liu P, Tao J, Cai Y, Pan H, Xu X, Tang RK. Role of fetal bovine serum in the prevention of calcification in biological fluids. J Cryst Growth 2008;310:4672–5.
[285] Chaudhary LR, Hofmeister AM, Hruska KA. Differential growth factor control of bone formation through osteoprogenitor differentiation. Bone 2004;34:402–11.
[286] Greenwald I. The effect of phosphate on the solubility of calcium carbonate and of bicarbonate on the solubility of calcium and magnesium phosphates. J Biol Chem 1945;161:697–704.
[287] Gron P, Spinelli M, Trautz O, Brudevold F. The effect of carbonate on the solubility of hydroxylapatite. Arch Oral Biol 1963;8:251–63.
[288] Kim HM, Kim YS, Woo KM, Park SJ, Rey C, Kim Y, et al. Dissolution of poorly crystalline apatite crystals by osteoclasts determined on artificial thin-film apatite. J Biomed Mater Res 2001;56:250–6.
[289] Leeuwenburgh S, Layrolle P, Barrere F, de Bruijn J, Schoonman J, van Blitterswijk CA, et al. Osteoclastic resorption of biomimetic calcium phosphate coatings in vitro. J Biomed Mater Res 2001;56:208–15.
[290] Logan MA, Taylor HL. Solubility of bone salt. III. Partial solution of bone and carbonate-containing calcium phosphate precipitates. J Biol Chem 1938;125:391–7.
[291] Bachra BN, Trautz OR. Carbonic anhydrase and the precipitation of apatite. Science 1962;137:337–8.
[292] Bachra BN, Trautz OR, Simon SL. Precipitation of calcium carbonates and phosphates. I. Spontaneous precipitation of calcium carbonates and phosphates under physiological conditions. Arch Biochem Biophys 1963;103:124–38.
[293] Bachra BN. Precipitation of calcium carbonates and phosphates from metastable solutions. Ann NY Acad Sci 1963;109:251–5.
[294] Bachra BN, Trautz OR, Simon SL. Precipitation of calcium carbonates and phosphates. III. The effect of magnesium and fluoride ions on the spontaneous precipitation of calcium carbonates and phosphates. Arch Oral Biol 1965;10:731–8.
[295] Posner AS, Fairy C, Dallemagne CJ. Defect apatite series in synthetic and natural calcium phosphates: the concept of pseudoapatites. Biochim Biophys Acta 1954;15:304–5.
[296] Eanes ED, Gillessen IH, Posner AS. Intermediate states in the precipitation of hydroxyapatite. Nature 1965;208:365–7.
[297] Bachra BN, Sobel AE, Stanford JW. Calcification. XXIV. Mineralization of collagen and other fibers. Arch Biochem Biophys 1959;84:79–95.
[298] Bachra BN, Sobel AE. Calcification. XXV. Mineralization of reconstituted collagen. Arch Biochem Biophys 1959;85:9–18.
[299] Goldenberg H, Sobel AE. Calcification. 9. Influence of alkaline earths on survival of the calcifying mechanism. Proc Soc Exp Biol Med 1952;81:695–8.
[300] Okazaki M, Moriwaki Y, Aoba T, Doi Y, Takahashi J, Kimura H. Crystallinity changes of CO_3-apatites in solutions at physiological pH. Caries Res 1982;16:308–14.
[301] Termine JD, Eanes ED, Conn KM. Phosphoprotein modulation of apatite crystallization. Calcif Tissue Int 1980;31:247–51.
[302] Kokubo T, Ito S, Shigematsu M, Sakka S, Yamamuro T. Fatigue and life-time of bioactive glass-ceramic A–W containing apatite and wollastonite. J Mater Sci 1987;22:4067–70.
[303] Web of Knowledge[SM]. Thomson Reuters, November 2013.
[304] Kokubo T, Takadama H. How useful is SBF in predicting in vivo bone bioactivity. Biomaterials 2006;27:2907–15.
[305] ISO 23317, Implants for surgery – in vitro evaluation for apatite-forming ability of implant materials; 2007.
[306] Pan H, Zhao X, Darvell BW, Lu WW. Apatite-formation ability – predictor of "bioactivity?". Acta Biomater 2010;6:4181–8.
[307] Bohner M, Lemaitre J. Can bioactivity be tested in vitro with SBF solution? Biomaterials 2009;30:2175–9.
[308] Oyane A, Onuma K, Kokubo T, Ito A. Clustering of calcium phosphate in the system $CaCl_2$–H_3PO_4–KCl–H_2O. J Phys Chem B 1999;103:8230–5.
[309] Yin X, Stott MJ. Biological calcium phosphates and Posner's cluster. J Phys Chem 2003;118:3717–23.
[310] Habraken WJEM, Tao JH, Brylka LJ, Friedrich H, Bertinetti L, Schenk AS, et al. Ion-association complexes unite classical and non-classical theories for the biomimetic nucleation of calcium phosphate. Nat Commun 2013;4:1507.
[311] Tsuru K, Kubo M, Hayakawa S, Ohtsuki C, Osaka A. Kinetics of apatite deposition on silica gel dependent on the inorganic ion composition of simulated body fluids. J Ceram Soc Jpn 2001;109:412–8.
[312] Spanos N, Misirlis DY, Kanellopoulou DG, Koutsoukos PG. Seeded growth of hydroxyapatite in simulated body fluid. J Mater Sci 2006;41:1805–12.
[313] Hashizume M, Nagasawa Y, Suzuki T, Kawashima S, Kamitakahara M. Effect of preparative conditions on crystallinity of apatite particles obtained from simulated body fluids. Colloid Surface B 2011;84:545–9.
[314] Sigel H, Scheller KH, Prijs B. Metal ion/buffer interactions. Stability of alkali and alkaline earth ion complexes with triethanolamine (Tea), 2-amino-2(hydroxymethyl)-1,3-propanediol (Tris) and 2-[bis(2-hydroxyethyl)-amino]2(hydroxymethyl)-1,3-propanediol (Bistris) in aqueous and mixed solvents. Inorg Chim Acta 1982;66:147–55.
[315] Serro AP, Saramago B. Influence of sterilization on the mineralization of titanium implants induced by incubation in various biological model fluids. Biomaterials 2003;24:4749–60.
[316] Rohanova D, Boccaccini AR, Yunos DM, Horkavcova D, Brezovska I, Helebrant A. Tris buffer in simulated body fluid distorts the assessment of glass-ceramic scaffold bioactivity. Acta Biomater 2011;7:2623–30.

[317] Du C, Klasens P, Haan RE, Bezemer J, Cui FZ, de Groot K, et al. Biomimetic calcium phosphate coatings on Polyactive® 1000/70/30. J Biomed Mater Res 2002;59:535–46.
[318] Barrere F, van der Valk CM, Meijer G, Dalmeijer RAJ, de Groot K, Layrolle P. Osteointegration of biomimetic apatite coating applied onto dense and porous metal implants in femurs of goats. J Biomed Mater Res 2003;67B:655–65.
[319] Wang J, Layrolle P, Stigter M, de Groot K. Biomimetic and electrolytic calcium phosphate coatings on titanium alloy: physicochemical characteristics and cell attachment. Biomaterials 2004;25:583–92.
[320] Habibovic P, van der Valk CM, van Blitterswijk CA, de Groot K. Influence of octacalcium phosphate coating on osteoinductive properties of biomaterials. J Mater Sci Mater Med 2004;15:373–80.
[321] Chou YF, Chiou WA, Xu Y, Dunn JCY, Wu BM. The effect of pH on the structural evolution of accelerated biomimetic apatite. Biomaterials 2004;25:5323–31.
[322] Chen Y, Mak AFT, Li J, Wang M, Shum AWT. Formation of apatite on poly(α-hydroxy acid) in an accelerated biomimetic process. J Biomed Mater Res 2005;73B:68–76.
[323] Li X, Xie J, Yuan X, Xia Y. Coating electrospun poly(ε-caprolactone) fibers with gelatin and calcium phosphate and their use as biomimetic scaffolds for bone tissue engineering. Langmuir 2008;24:14145–50.
[324] Yang F, Wolke JGC, Jansen JA. Biomimetic calcium phosphate coating on electrospun poly(ε-caprolactone) scaffolds for bone tissue engineering. Chem Eng J 2008;137:154–61.
[325] Kim HM, Miyazaki T, Kokubo T, Nakamura T. Revised simulated body fluid. Key Eng Mater 2000;192:47–50.
[326] Oyane A, Kim HM, Furuya T, Kokubo T, Miyazaki T, Nakamura T. Preparation and assessment of revised simulated body fluids. J Biomed Mater Res 2003;65A:188–95.
[327] Oyane A, Onuma K, Ito A, Kim HM, Kokubo T, Nakamura T. Formation and growth of clusters in conventional and new kinds of simulated body fluids. J Biomed Mater Res 2003;64A:339–48.
[328] Jalota S, Bhaduri SB, Tas AC. Effect of carbonate content and buffer type on calcium phosphate formation in SBF solutions. J Mater Sci Mater Med 2006;17:697–707.
[329] Su XL, Nie LH, Yao SZ. A novel gas-diffusion/flow-injection system coupled with a bulk acoustic wave impedance sensor for total inorganic carbonate and its application to determination of total inorganic and total organic carbon in waters. Anal Chim Acta 1997;349:143–51.
[330] Yun YS, Lee SB, Park JM, Lee CI, Yang JW. Carbon dioxide fixation by algal cultivation using wastewater nutrients. J Chem Tech Biotechnol 1997;69:451–5.
[331] Quatrehomme G, Bolla M, Muller M, Rocca JP, Grevin G, Bailet P, et al. Experimental single controlled study of burned bones: contribution of scanning electron microscopy. J Forensic Sci 1998;43:417–22.
[332] Ubelaker DH. The forensic evaluation of burned skeletal remains: a synthesis. Forensic Sci Int 2009;183:1–5.
[333] Koustova E, Stanton K, Gushchin V, Alam HB, Stegalkina S, Rhee PM. Effects of lactated Ringer's solutions on human leukocytes. J Trauma 2002;52:872–8.
[334] Nijhuis AWG, Leeuwenburgh SCG, Jansen JA. Wet-chemical deposition of functional coatings for bone implantology. Macromol Biosci 2010;10:1316–29.
[335] Grondahl L, Cardona F, Cheim K, Wentrup-Byrne E. Calcium phosphate nucleation on surface-modified PTFE membranes. J Mater Sci Mater Med 2003;14:503–10.
[336] Kolos EC, Ruys AJ, Rohanizadeh R, Muir MM, Roger G. Calcium phosphate fibers synthesized from a simulated body fluid. J Mater Sci Mater Med 2006;17:1179–89.
[337] Shi S, Chen S, Zhang X, Shen W, Li X, Hu W, et al. Biomimetic mineralization synthesis of calcium-deficient carbonate-containing hydroxyapatite in a three-dimensional network of bacterial cellulose. J Chem Technol Biotechnol 2009;84:285–90.
[338] Rodriguez K, Renneckar S, Gatenholm P. Biomimetic calcium phosphate crystal mineralization on electrospun cellulose-based scaffolds. Appl Mater Interfaces 2011;3:681–9.
[339] Jalota S, Bhaduri SB, Tas AC. In vitro testing of calcium phosphate (HA, TCP and biphasic HA–TCP) whiskers. J Biomed Mater Res 2006;78A:481–90.
[340] Wang K, Leng Y, Lu X, Ren F. Calcium phosphate bioceramics induce mineralization modulated by proteins. Mater Sci Eng C 2013;33:3245–55.
[341] Song J, Saiz E, Bertozzi CR. A new approach to mineralization of biocompatible hydrogel scaffolds: an efficient process toward 3-dimensional bonelike composites. J Am Chem Soc 2003;125:1236–43.
[342] Libouban H, Filmon R, Maureac A, Basle MF, Chappard D. Fetuin and osteocalcin interact with calcospherite formation during the calcification process of poly(2-hydroxyethylmethacrylate) in vitro: a Raman microspectroscopic monitoring. J Raman Spectrosc 2009;40:1234–9.
[343] Takadama H, Kim HM, Kokubo T, Nakamuta T. Mechanism of biomineralization of apatite on a sodium-silicate glass: TEM–EDX study in vitro. Chem Mater 2001;13:1108–13.
[344] Prakash KH, Kumar R, Yu SC, Khor KA, Cheang P. On the kinetics of apatite growth on substrates under physiological conditions. Langmuir 2006;22:269–76.
[345] Tarasevich BJ, Chusuei CC, Allara DL. Nucleation and growth of calcium phosphate from physiological solutions onto self-assembled templates by a solution-formed nucleus mechanism. J Phys Chem B 2003;107:10367–77.
[346] Liu X, Fu RKY, Poon RWY, Chen P, Chu PK, Ding C. Biomimetic growth of apatite on hydrogen-implanted silicon. Biomaterials 2004;25:5575–81.
[347] Toworfe GK, Composto RJ, Shapiro IM, Ducheyne P. Nucleation and growth of calcium phosphate on amine-, carboxyl- and hydroxyl-silane self-assembled monolayers. Biomaterials 2006;27:631–42.
[348] Baskar D, Balu R, Kumar TSS. Mineralization of pristine chitosan film through biomimetic process. Int J Biol Macromol 2011;49:385–9.
[349] Brown JL, Nair LS, Bender J, Allcock HR, Laurencin CT. The formation of an apatite coating on carboxylated polyphosphazenes via a biomimetic process. Mater Lett 2007;61:3692–5.
[350] Cauda V, Argyo C, Bein T. Impact of different PEGylation patterns on the long-term bio-stability of colloidal mesoporous silica nanoparticles. J Mater Chem 2010;20:8693–9.
[351] Pribosic I, Klopcic SB, Kosmac T. Biomimetic preparation and characterization of bioactive coatings on alumina and zirconia ceramics. J Am Ceram Soc 2010;93:288–94.
[352] Miyaji F, Kim HM, Handa S, Kokubo T, Nakamura T. Bonelike apatite coating on organic polymers: novel nucleation process using sodium silicate solution. Biomaterials 1999;20:913–9.
[353] Akazawa T, Murata M, Hino J, Nagano F, Shigyo T, Nomura T, et al. Surface structure and biocompatibility of demineralized dentin matrix granules soaked in a simulated body fluid. Appl Surf Sci 2012;262:51–5.
[354] Muzquiz-Ramos EM, Cortes-Hernandez DA, Escobedo-Bocardo J. Biomimetic apatite coating on magnetite particles. Mater Lett 2010;64:1117–9.
[355] Sailaja GS, Sreenivasan K, Yokogawa Y, Kumary TV, Varma HK. Bioinspired mineralization and cell adhesion on surface functionalized poly(vinyl alcohol) films. Acta Biomater 2009;5:1647–55.
[356] Will J, Hoppe A, Muller FA, Raya CT, Fernandez JM, Greil P. Bioactivation of biomorphous silicon carbide bone implants. Acta Biomater 2010;6:4488–94.
[357] Pittrof A, Bauer S, Schmuki P. Micropatterned TiO_2 nanotube surfaces for site-selective nucleation of hydroxyapatite from simulated body fluid. Acta Biomater 2011;7:424–31.
[358] Uetsuki K, Kaneda H, Shirosaki Y, Hayakawa S, Osaka A. Effects of UV-irradiation on in vitro apatite-forming ability of TiO_2 layers. Mater Sci Eng B 2010;173:213–5.
[359] Chu CL, Pu YP, Yin LH, Chung CY, Yeung KWK, Chu PK. Biomimetic deposition process of an apatite coating on NiTi shape memory alloy. Mater Lett 2006;60:3002–6.
[360] Takeuchi A, Ohtsuki C, Miyazaki T, Tanaka H, Yamazaki M, Tanihara M. Deposition of bone-like apatite on silk fiber in a solution that mimics extracellular fluid. J Biomed Mater Res 2003;65A:283–9.
[361] Iimori Y, Kameshima Y, Yasumori A, Okada K. Effect of solid/solution ratio on apatite formation from $CaSiO_3$ ceramics in simulated body fluid. J Mater Sci Mater Med 2004;14:1247–53.
[362] Tavangarian F, Emadi R. Nanostructure effects on the bioactivity of forsterite bioceramic. Mater Lett 2011;65:740–3.
[363] Ning CQ, Zhou Y. In vitro bioactivity of a biocomposite fabricated from HA and Ti powders by powder metallurgy method. Biomaterials 2002;23:2909–15.
[364] Aryal S, Bhattarai SR, Bahadur RKC, Khil MS, Lee DR, Kim HY. Carbon nanotubes assisted biomimetic synthesis of hydroxyapatite from simulated body fluid. Mater Sci Eng A 2006;426:202–7.
[365] Filgueiras MR, La Torre G, Hench LL. Solution effects on the surface reactions of a bioactive glass. J Biomed Mater Res 1993;27:445–53.
[366] Pirayesh H, Nychka JA. Sol–gel synthesis of bioactive glass-ceramic 45S5 and its in vitro dissolution and mineralization behavior. J Am Ceram Soc 2013;96:1643–50.
[367] Gu XN, Zhou WR, Zheng YF, Cheng Y, Wei SC, Zhong SP, et al. Corrosion fatigue behaviors of two biomedical Mg alloys – AZ91D and WE43 – in simulated body fluid. Acta Biomater 2010;6:4605–13.
[368] Lorenz C, Brunner JG, Kollmannsberger P, Jaafar L, Fabry B, Virtanen S. Effect of surface pre-treatments on biocompatibility of magnesium. Acta Biomater 2009;5:2783–9.
[369] Ichibouji T, Miyazaki T, Ishida E, Sugino A, Ohtsuki C. Apatite mineralization abilities and mechanical properties of covalently cross-linked pectin hydrogels. Mater Sci Eng C 2009;29:1765–9.
[370] Oyane A, Ootsuka T, Hayama K, Sogo Y, Ito A. Enhanced immobilization of acidic proteins in the apatite layer via electrostatic interactions in a supersaturated calcium phosphate solution. Acta Biomater 2011;7:2969–76.
[371] Zhong C, Chu CC. Biomimetic mineralization of acid polysaccharide-based hydrogels: towards porous 3-dimensional bone-like biocomposites. J Mater Chem 2012;22:6080–7.
[372] Aoba T, Shimazu Y, Taya Y, Soeno Y, Sato K, Miake Y. Fluoride and apatite formation in vivo and in vitro. J Electron Microsc 2003;52:615–25.
[373] Wang CG, Liao JW, Gou BD, Huang J, Tang RK, Tao JH, et al. Crystallization at multiple sites inside particles of amorphous calcium phosphate. Cryst Growth Des 2009;9:2620–6.
[374] Wheeler EJ, Lewis D. An X-ray study of the paracrystalline nature of bone apatite. Calcif Tiss Res 1977;24:243–8.
[375] Patterson AL. The Scherrer formula for X-ray particle size determination. Phys Rev 1939;56:978–82.
[376] Warren BE, Averbach BL. The effect of cold-work distortion on X-ray patterns. J Appl Phys 1950;21:595–9.
[377] Venkateswarlu K, Bose AC, Rameshbabu N. X-ray peak broadening studies of nanocrystalline hydroxyapatite by Williamson–Hall analysis. Phys B 2010;405:4256–61.

[378] Sudarsanan K, Young RA. Significant precision in crystal structural details: Holly Springs hydroxyapatite. Acta Crystallogr 1969;B25:1534–43.
[379] Wen HB, Wolke JGC, de Wijn JR, Liu Q, Cui FZ, de Groot K. Fast precipitation of calcium phosphate layers on titanium induced by simple chemical treatments. Biomaterials 1997;18:1471–8.
[380] Wen HB, de Wijn JR, Liu Q, de Groot K, Cui FZ. A simple method to prepare calcium phosphate coatings on Ti6Al4V. J Mater Sci Mater Med 1997;8:765–70.
[381] Zhang J, Nancollas GH. Kinetics and mechanisms of octacalcium phosphate dissolution at 37 °C. J Phys Chem 1992;96:5478–83.
[382] Suzuki O. Octacalcium phosphate: osteoconductivity and crystal chemistry. Acta Biomater 2010;6:3379–87.
[383] Tas AC. Granules of brushite and octacalcium phosphate from marble. J Am Ceram Soc 2011;94:3722–6.
[384] Radin SR, Ducheyne P. The effect of calcium phosphate ceramic composition and structure on in vitro behavior. II. Precipitation. J Biomed Mater Res 1993;27:35–45.
[385] Wootton R, Reeve J, Veall N. Skeletal blood flow and calcium kinetics in metabolic bone disease. Calcif Tiss Res 1977;22:325–8.
[386] Lee S, Ishibashi S, Shimomura Y, Katsuura T. Physiological functions of the effects of the different bathing method on recovery from local muscle fatigue. J Physiol Anthropol 2012;31:26.
[387] Rochette CN, Rosenfeldt S, Heiss A, Narayanan T, Ballauff M, Jahnen-Dechent W. A shielding topology stabilizes the early stage protein–mineral complexes of fetuin-A and calcium phosphate: a time-resolved small-angle X-ray study. ChemBioChem 2009;10:735–40.
[388] Cantaert B, Beniash E, Meldrum FC. The role of poly(aspartic acid) in the precipitation of calcium phosphate in confinement. J Mater Chem B 2013;1:6586–95.
[389] He G, Dahl T, Veis A, George A. Nucleation of apatite crystals in vitro by self-assembled dentin matrix protein 1. Nat Mater 2003;2:552–8.
[390] Tsuji T, Onuma K, Yamamoto A, Iijima M, Shiba K. Direct transformation from amorphous to crystalline calcium phosphate facilitated by motif-programmed artificial proteins. PNAS 2008;105:16866–70.
[391] Kwak SY, Green S, Wiedemann-Bidlack FB, Beniash E, Yamakoshi Y, Simmer JP, et al. Regulation of calcium phosphate formation by amelogenins under physiological conditions. Eur J Oral Sci 2011;119(Suppl. 1):103–11.
[392] Ibasco S, Tamimi F, Meszaros R, Le Nihouannen D, Vengallatore S, Harvey E, et al. Magnesium-sputtered titanium for the formation of bioactive coatings. Acta Biomater 2009;5:2338–47.
[393] Kurtulus G, Tas AC. Transformations of neat and heated struvite ($MgNH_4PO_4{\cdot}6H_2O$). Mater Lett 2011;65:2883–6.
[394] Ryall RL. The future of stone research: rummagings in the attic, Randall's plaque, nanobacteria, and lessons from phylogeny. Urol Res 2008;36:77–97.
[395] Torzewska A, Staczek P, Rozalski A. Crystallization of urine mineral components may depend on the chemical nature of Proteus endotoxin polysaccharides. J Med Microbiol 2003;52:471–7.
[396] Griffith DP, Musher DM, Itin C. Urease – primary cause of infection-induced urinary stones. Invest Urol 1976;13:346–50.
[397] Prywer J, Torzewska A. Bacterially induced struvite growth from synthetic urine: experimental and theoretical characterization of crystal morphology. Cryst Growth Des 2009;9:3538–43.
[398] Gron P, Hay DI. Inhibition of calcium phosphate precipitation by human salivary secretions. Arch Oral Biol 1976;21:201–5.
[399] Nancollas GH. The involvement of calcium phosphates in biological mineralization and demineralization processes. Pure Appl Chem 1992;64:1673–8.
[400] Johansson BI, Lemons JE, Hao SQ. Corrosion of dental copper, nickel, and gold alloys in artificial saliva and saline solutions. Dent Mater 1989;5:324–8.
[401] Fusayama T, Nomoto S, Katayori T. Corrosion of gold and amalgam placed in contact with each other. J Dent Res 1963;42:1183–97.
[402] Shellis RP, Heywood BR, Wahab FK. Formation of brushite, monetite and whitlockite during equilibration of human enamel with acid solutions at 37 °C. Caries Res 1997;31:71–7.
[403] Dickens SH, Flaim GM, Takagi S. Mechanical properties and biochemical activity of remineralizing resin-based Ca-PO_4 cements. Dent Mater 2003;19:558–66.
[404] Lippert F. Dose–response effects of zinc and fluoride on caries lesion remineralization. Caries Res 2012;46:62–8.
[405] Efflandt SE, Cook RF, Francis LF. Apatite growth on bioactive glass in artificial saliva. MRS Proc 2000;662(LL2):5.
[406] Leung VWH, Darvell BW. Artificial salivas for in vitro studies of dental materials. J Dent 1997;25:475–84.
[407] Marques MRC, Loebenberg R, Almukainzi M. Simulated biological fluids with possible application in dissolution testing. Dissolut Technol 2011;18:15–28.
[408] Campbell J, Wathen N, MacIntosh M, Cass P, Chard T. Biochemical composition of the amniotic fluid and extraembryonic coelomic fluid in the first trimester of pregnancy. Br J Obstet Gynaec 1992;99:563–5.
[409] Pettit BR, Baker SP, King GS. The composition of amniotic fluid in pregnancies complicated by fetal anencephaly or spina bifida. Br J Obstet Gynaec 1979;86:637–41.
[410] MacDonald I. Chemical analysis of human foetal skull bones. Biochem J 1954;57:437–9.
[411] Kim KS, Cho CH, Kim YS, Yoon KS, Jung MH, Park HK. Characterization of ultrastructure and collagen composition of the teratoma membrane: comparison to the amniotic membrane. Microsc Res Techniq 2013;76:432–41.
[412] Dorozhkina EI, Dorozhkin SV. Structure and properties of the precipitates formed from the condensed solutions of the revised simulated body fluid. J Biomed Mater Res 2003;67A:578–81.
[413] Chatzistavrou X, Tsigkou O, Amin HD, Paraskevopoulos KM, Salih V, Boccaccini AR. Sol–gel based fabrication and characterization of new bioactive glass-ceramic composites for dental applications. J Eur Ceram Soc 2012;32:3051–61.
[414] Allo BA, Rizkalla AS, Mequanint K. Hydroxyapatite formation on sol–gel derived poly(ε-caprolactone)/bioactive glass hybrid biomaterials. ACS Appl Mater Interfaces 2012;4:3148–56.
[415] Roohani-Esfahani SI, Lu ZF, Li JJ, Ellis-Behnke R, Kaplan DL, Zreiqat H. Effect of self-assembled nanofibrous silk/polycaprolactone layer on the osteoconductivity and mechanical properties of biphasic calcium phosphate scaffolds. Acta Biomater 2012;8:302–12.
[416] Vroman L. Finding seconds count after contact with blood (and that is all I did). Colloid Surface B 2008;62:1–4.
[417] Kulkarni SA, Feng SS. Effects of particle size and surface modification on cellular uptake and biodistribution of polymeric nanoparticles for drug delivery. Pharm Res 2013;30:2512–22.
[418] Piacentini C, Marchetti C, Callegari A, Setti M, Bernasconi G, Baciliero U, et al. Endoarticular loose bodies and calcifications of the disk of the temporomandibular joint: morphological features and chemical composition. Scanning Microsc 1995;9:789–96.
[419] Yu JK, Pan H, Huang SM, Huang NL, Yao CC, Hsiao KM, et al. Calcium content of different compositions of gallstones and pathogenesis of calcium carbonate gallstones. Asian J Surg 2013;36:26–35.
[420] Palchik NA, Moroz TN. Polymorph modifications of calcium carbonate in gallstones. J Cryst Growth 2005;283:450–6.
[421] Wentrup-Byrne E, Chua-Anusorn W, St. Pierre ST, Webb J, Ramsay A, Rintoul L. A spectroscopic study of thalassemic gallstones. Biospectroscopy 1997;3:409–16.